Inorg. Chem. **2002**, *41*, 6307–6321

Copper Chemistry of β-Diketiminate Ligands: Monomer/Dimer Equilibria and a New Class of Bis(μ-oxo)dicopper Compounds

Douglas J. E. Spencer,[†] Anne M. Reynolds,[†] Patrick L. Holland,[†] Brian A. Jazdzewski,[†] Carole Duboc-Toia,[†,‡] Laurent Le Pape,[§] Seiji Yokota,[||] Yoshimitsu Tachi,[||] Shinobu Itoh,*[,||] and William B. Tolman*[,†]

Department of Chemistry and Center for Metals in Biocatalysis, University of Minnesota, 207 Pleasant Street SE, Minneapolis, Minnesota 55455, Laboratoire des Champs Magnetiques Intenses, 25 Av. des Martyrs, BP 166, CEA-Grenoble, F-38042 Grenoble Cedex 9, France, Laboratoire de Physico-chimie des Métaux en Biologie, FRE 2427 CEA-CNRS-UJF, Département Réponse et Dynamique Cellulaires, CEA-Grenoble, 38054 Grenoble Cedex 9, France, and Department of Chemistry, Graduate School of Science, Osaka City University, 3-3-138 Sugimoto, Sumiyoshi-ku, Osaka 558-8585, Japan

Received May 29, 2002

A series of Cu(I) and Cu(II) complexes of a variety of β-diketiminate ligands (L^-) with a range of substitution patterns were prepared and characterized by spectroscopic, electrochemical, and, in several cases, X-ray crystallographic methods. Specifically, complexes of the general formula $[LCuCl]_2$ were structurally characterized and their magnetic properties assessed through EPR spectroscopy of solutions and, in one instance, by variable-temperature SQUID magnetization measurements on a powder sample. UV–vis spectra indicated reversible dissociation to 3-coordinate monomers LCuCl in solution at temperatures above –55 °C. The Cu(I) complexes LCu(MeCN) exhibited reversible Cu(I)/Cu(II) redox couples with $E_{1/2}$ values between +300 and +520 mV versus NHE (cyclic voltammetry, MeCN solutions). These complexes were highly reactive with O_2, yielding intermediates that were identified as rare examples of neutral bis(μ-oxo)dicopper complexes on the basis of their EPR silence, diagnostic UV–vis absorption data, and O-isotope-sensitive resonance Raman spectroscopic features. The structural features of the compounds $[LCuCl]_2$ and LCu(MeCN) as well as the proclivity to form bis(μ-oxo)dicopper products upon oxygenation of the Cu(I) complexes are compared to data previously reported for complexes of more sterically hindered β-diketiminate ligands (Aboelella, N. W.; Lewis, E. A.; Reynolds, A. M.; Brennessel, W. W.; Cramer, C. J.; Tolman, W. B. *J. Am. Chem. Soc.* **2002**, *124*, 10600. Spencer, D. J. E.; Aboelella, N. W.; Reynolds, A. M.; Holland, P. L.; Tolman, W. B. *J. Am. Chem. Soc.* **2002**, *124*, 2108. Holland, P. L.; Tolman, W. B. *J. Am. Chem. Soc.* **1999**, *121*, 7270). The observed structural and reactivity differences are rationalized by considering the steric influences of both the substituents on the flanking aromatic rings and those present on the β-diketiminate backbone.

Introduction

Understanding the nature of reactive intermediates that form upon reaction of O_2 with Cu(I) centers in proteins is critical for developing structure/function relationships in metallobiochemistry and catalysis.[1] Considerable progress toward this goal has been attained through examination of the dioxygen reactivity of synthetic Cu(I) complexes, which has resulted in the characterization of a variety of biologically relevant superoxo, μ-peroxo, and bis(μ-oxo) copper complex topologies (cf. Figure 1).[2] A key research objective has been to comprehend how supporting ligand structural features influence the relative stabilities and interconversions of these species, with recent emphasis on ligand effects on the

* To whom correspondence should be addressed. E-mail: shinobu@scisv.sci.osaka-cu.ac.jp (S.I.); tolman@chem.umn.edu (W.B.T.). Fax: 612-624-7029 (W.B.T.).
[†] University of Minnesota.
[‡] Laboratoire des Champs Magnetiques Intenses, CEA-Grenoble.
[§] Laboratoire de Physico-chimie des Métaux en Biologie, CEA-Grenoble.
[||] Osaka City University.

(1) (a) Solomon, E. I.; Sundaram, U. M.; Machonkin, T. E. *Chem. Rev.* **1996**, *96*, 2563−2605. (b) Klinman, J. P. *Chem. Rev.* **1996**, *96*, 2541−2561. (c) Solomon, E. I.; Chen, P.; Metz, M.; Lee, S.-K.; Palmer, A. E. *Angew. Chem., Int. Ed.* **2001**, *40*, 4570−4590.

10.1021/ic020369k CCC: $22.00
Published on Web 11/08/2002

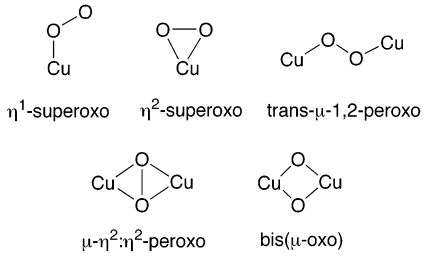

Figure 1. Observed geometries of mono- and dicopper intermediates formed in reactions of Cu(I) complexes with O_2.

equilibrium between (μ-η^2:η^2-peroxo)dicopper(II,II) and bis(μ-oxo)dicopper(III,III) units[3] that are relevant to proposed metalloprotein active site intermediates.[1,4] We and others showed that both of these units could be supported by neutral, multidentate N-donor ligands and that ligand structural elements (e.g., size of substituents, macrocycle ring size, denticity) play a critical role in determining which unit(s) formed and how it (they) reacted.[2,3,5] More recently, we began to examine the O_2 reactivity of Cu(I) complexes of β-diketiminate ligands, which have been used extensively in coordination chemistry[6] and have been applied lately toward the isolation of novel low-coordinate metalloprotein active site models comprising Cu(II)[7] and Fe(I or II).[8] In preliminary communications,[9] the characterization of novel monomeric

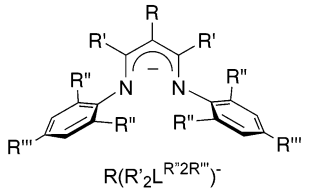

R	R′	R″	R‴
H	Me	Me	H
H	Me	Et	H
H	Me	iPr	H
Ph	H	Me	H
Ph	H	Et	H
Ph	H	iPr	H
3,5-$(CF_3)_2C_6H_3$	H	Me	H
3,5-$(CF_3)_2C_6H_3$	H	Et	H
3,5-$(CF_3)_2C_6H_3$	H	iPr	H
NO_2	H	Me	Me
Cl	Me	Me	H

Figure 2. β-Diketiminate ligands used in this work, with the abbreviation system indicated. Note that when R‴ = H, this substituent will be omitted from the ligand abbreviation (e.g. $H(Me_2L^{iPr2})^-$ for R = H, R′ = Me, R″ = ^{i}Pr, and R‴ = H).

1:1 O_2 adducts or bis(μ-oxo)dicopper compounds supported by β-diketiminates comprising identical 2,6-diisopropylphenyl flanking groups but disparate backbone substituents, $H(R'_2L^{iPr2})^-$ (R′ = Me or ^{t}Bu) and $Ph(H_2L^{iPr2})^-$, respectively, were described (see Figure 2 for ligand abbreviation scheme).

Herein, we report the results of studies of the Cu(I) and Cu(II) chemistry of an expanded set of β-diketiminates with variable substituent arrays. An analysis of the structures of complexes of the general formula $[LCuCl]_n$ (n = 1 or 2) and LCu(MeCN) has shed light on the steric effects of the

(2) Recent reviews: (a) Blackman, A. G.; Tolman, W. B. In *Metal-Oxo and Metal-Peroxo Species in Catalytic Oxidations*; Meunier, B., Ed.; Springer-Verlag: Berlin, 2000; Vol. 97, pp 179−211. (b) Kopf, M.-A.; Karlin, K. D. In *Biomimetic Oxidations Catalyzed by Transition Metal Complexes*; Meunier, B., Ed.; Imperial College Press: London, 2000; pp 309−362. (c) Karlin, K. D.; Zuberbühler, A. D. In *Bioinorganic Catalysis*, 2nd ed.; Reedijk, J., Ed.; Marcel Dekker: New York, 1999; pp 469−534. (d) Mahadevan, V.; Gebbink, R. J. M. K.; Stack, T. D. P. *Curr. Opin. Chem. Biol.* **2000**, *4*, 228−234. (e) Que, L., Jr.; Tolman, W. B. *Angew. Chem., Int. Ed.* **2002**, *41*, 1114−1137.

(3) (a) Tolman, W. B. *Acc. Chem. Res.* **1997**, *30*, 227−237. (b) Holland, P. L.; Tolman, W. B. *Coord. Chem. Rev.* **1999**, *190*−*192*, 855−869. (c) Mahadevan, V.; Henson, M. J.; Solomon, E. I.; Stack, T. D. P. *J. Am. Chem. Soc.* **2000**, *122*, 10249−10250. (d) Lam, B. M. T.; Halfen, J. A.; Young, V. G., Jr.; Hagadorn, J. R.; Holland, P. L.; Lledós, A.; Cucurull-Sánchez, L.; Novoa, J. J.; Alvarez, S.; Tolman, W. B. *Inorg. Chem.* **2000**, *39*, 4059−4072. (e) Cahoy, J.; Holland, P. L.; Tolman, W. B. *Inorg. Chem.* **1999**, *38*, 2161−2168. (f) Pidcock, E.; DeBeer, S.; Obias, H. V.; Hedman, B.; Hodgson, K. O.; Karlin, K. D.; Solomon, E. I. *J. Am. Chem. Soc.* **1999**, *121*, 1870−1878. (g) Obias, H. V.; Lin, Y.; Murthy, N. N.; Pidcock, E.; Solomon, E. I.; Ralle, M.; Blackburn, N. J.; Neuhold, Y.-M.; Zuberbühler, A. D.; Karlin, K. D. *J. Am. Chem. Soc.* **1998**, *120*, 12960−12961. (h) Hayashi, H.; Fujinami, S.; Nagatomo, S.; Ogo, S.; Suzuki, M.; Uehara, A.; Watanabe, Y.; Kitagawa, T. *J. Am. Chem. Soc.* **2000**, *122*, 2124−2125. (i) Liang, H.-C.; Zhang, C. X.; Henson, M. J.; Sommer, R. D.; Hatwell, K. R.; Kaderli, S.; Zuberbühler, A. D.; Rheingold, A. L.; Solomon, E. I.; Karlin, K. D. *J. Am. Chem. Soc.* **2002**, *124*, 4170−4171. (j) Hayashi, H.; Uozumi, K.; Fujinami, S.; Nagatomo, S.; Shiren, K.; Furutachi, H.; Suzuki, M.; Uehara, A.; Kitagawa, T. *Chem. Lett.* **2002**, 416−417.

(4) (a) Decker, H.; Dillinger, R.; Tuczek, F. *Angew. Chem., Int. Ed.* **2000**, *39*, 1591−1595. (b) Holland, P. L.; Rodgers, K. R.; Tolman, W. B. *Angew. Chem., Int. Ed.* **1999**, *38*, 1139−1142.

(5) (a) Taki, M.; Itoh, S.; Fukuzumi, S. *J. Am. Chem. Soc.* **2001**, *123*, 6203−6204. (b) Itoh, S.; Kumei, H.; Taki, M.; Nagatomo, S.; Kitagawa, T.; Fukuzumi, S. *J. Am. Chem. Soc.* **2001**, *123*, 6708−6709. (c) Itoh, S.; Taki, M.; Nakao, H.; Holland, P. L.; Tolman, W. B.; L. Que, J.; Fukuzumi, S. *Angew. Chem., Int. Ed.* **2000**, *39*, 398−400. (d) Mahadevan, V.; DuBois, J. L.; Hedman, B.; Hodgson, K. O.; Stack, T. D. P. *J. Am. Chem. Soc.* **1999**, *121*, 5583−5584. (e) Pidcock, E.; Obias, H. V.; Abe, M.; Liang, H. C.; Karlin, K. D.; Solomon, E. I. *J. Am. Chem. Soc.* **1999**, *121*, 1299−1308. (f) Kodera, M.; Katayama, K.; Tachi, Y.; Kano, K.; Hirota, S.; Fujinami, S.; Suzuki, M. *J. Am. Chem. Soc.* **1999**, *121*, 11006−11007.

(6) Selected recent examples: (a) Kakliou, L.; Scanlon, W. J., IV; Qian, B.; Baek, S. W.; Smith, M. R., III. *Inorg. Chem.* **1999**, *38*, 5964−5977 and references therein. (b) Chamberlain, B. M.; Cheng, M.; Moore, D. R.; Ovitt, T. M.; Lobkovsky, E. B.; Coates, G. W. *J. Am. Chem. Soc.* **2001**, *123*, 3229−3238. (c) Stender, M.; Eichler, B. E.; Hardman, N. J.; Power, P. P.; Prust, J.; Noltemeyer, M.; Roesky, H. W. *Inorg. Chem.* **2001**, *40*, 2794−2799. (d) Hardman, N. J.; Power, P. P. *J. Am. Chem. Soc.* **2001**, *40*, 2474−2475. (e) MacAdams, L. A.; Kim, W.-K.; Liable-Sands, L. M.; Guzei, I. A.; Rheingold, A. L.; Theopold, K. H. *Organometallics* **2002**, *21*, 952−960. (f) Prust, J.; Hohmeister, H.; Stasch, A.; Roesky, H. W.; Magull, J.; Alexopoulos, E.; Usón, I.; Schmidt, H.-G.; Noltemeyer, M. *Eur. J. Inorg. Chem.* **2002**, 2156−2162. (g) Harder, S. *Organometallics* **2002**, *21*, 3782−3787.

(7) (a) Holland, P. L.; Tolman, W. B. *J. Am. Chem. Soc.* **1999**, *121*, 7270−7271. (b) Holland, P. L.; Tolman, W. B. *J. Am. Chem. Soc.* **2000**, *122*, 6331−6332. (c) Randall, D. W.; DeBeer, S.; Holland, P. L.; Hedman, B.; Hodgson, K. O.; Tolman, W. B.; Solomon, E. I. *J. Am. Chem. Soc.* **2000**, *122*, 11632−11648. (d) Jazdzewski, B. A.; Holland, P. L.; Pink, M.; Young, V. G., Jr.; Spencer, D. J. E.; Tolman, W. B. *Inorg. Chem.* **2001**, *40*, 6097−6107.

(8) (a) Smith, J. M.; Lachicotte, R. J.; Holland, P. L. *Chem. Commun.* **2001**, 1542−1543. (b) Smith, J. M.; Lachicotte, R. J.; Pittard, K. A.; Cundari, T. R.; Lukat-Rodgers, G.; Rodgers, K. R.; Holland, P. L. *J. Am. Chem. Soc.* **2001**, *123*, 9222−9223. (c) Andres, H.; Bominaar, E. L.; Smith, J. M.; Eckert, N. A.; Holland, P. L.; Münck, E. *J. Am. Chem. Soc.* **2002**, *124*, 3012−3025.

(9) (a) Spencer, D. J. E.; Aboelella, N. W.; Reynolds, A. M.; Holland, P. L.; Tolman, W. B. *J. Am. Chem. Soc.* **2002**, *124*, 2108−2809. (b) Aboelella, N. W.; Lewis, E. A.; Reynolds, A. M.; Brennessel, W. W.; Cramer, C. J.; Tolman, W. B. *J. Am. Chem. Soc.* **2002**, *124*, 10660−10661.

ligand substituent pattern. These effects are related to the reactivity of the Cu(I) species with O_2 at low temperature. For the β-diketiminates used here, rare examples of neutral bis(μ-oxo)dicopper complexes[10] are formed, which have been characterized by UV−vis, EPR, and resonance Raman spectroscopy. While this work was in progress, a Cu(I) complex of $H(Me_2L^{Me2})^-$ was reported to react with O_2 to yield a bis(μ-hydroxo)dicopper(II,II) complex, and the intermediacy of an unstable bis(μ-oxo) species was suggested.[11] In addition, a polymeric β-diketiminate Cu(I) species, $[NO_2(H_2L^{Me2Me})Cu]_n$,[12] a derived monomeric phosphine adduct,[12] and the oxidative degradation of Cu(II) and Zn(II) complexes of $H(Me_2L^{Me2Me})^-$ were described.[13]

Results and Discussion

Ligand Syntheses. A variety of β-diketimines with variable backbone and aryl substituents, $R(R'_2L^{R''2R'''})H$, were prepared to probe the influence of ligand structural variation on copper ion complexation and Cu(I)/O_2 chemistry (Figure 2). Of these, $NO_2(H_2L^{Me2Me})H$[12] and $H(Me_2L^{R''2})H$ (R″ = Me or Et)[14] were reported previously. The compound Cl(Me_2L^{Me2})H was prepared via the typical Schiff base condensation method,[6,15] here involving reaction of 2,6-dimethylaniline with 3-chloro-2,4-pentanedione. The syntheses of the remaining β-diketimines incorporating aryl units at the central backbone position began from the vinamidinium hexafluorophosphate salts derived from reaction of the appropriate arylacetic acid with $POCl_3$ and DMF at 70 °C (Scheme 1).[16,17] The salts were hydrolyzed by refluxing in a basic solution to give the respective dialdehydes (in enolized form) as brown oils. These brown oils were reacted without further purification with the appropriate aniline derivative to provide the desired β-diketimines, which were isolated as yellow crystalline solids. All new β-diketimines were characterized by ^{1}H and ^{13}C NMR spectroscopy, high-resolution mass spectrometry, and elemental analysis. Deprotonation with ^{n}BuLi in either pentane or THF yielded the lithium salts of the β-diketiminate ligands, which were isolated as solids for storage in the glovebox and subsequent use for preparing copper complexes. In some cases the salts retained a THF solvent molecule, as shown by ^{1}H and ^{13}C NMR spectroscopy.

Syntheses and Properties of Cu(II) Complexes. We prepared several Cu(II) complexes $[LCuCl]_2$ by treatment of selected lithium β-diketiminates with anhydrous $CuCl_2$·0.8THF,[18] where L = $H(Me_2L^{Et2})^-$, $Cl(Me_2L^{Me2})^-$, or $Ph(H_2L^{iPr2})^-$. X-ray crystal structures of the complexes comprising the first two ligands are shown in Figure 3, with crystallographic data and selected bond lengths and angles listed in Tables 1 and 2, respectively. Most notably, the diffraction data indicate dinuclear structures for the green compounds, which contain 4-coordinate Cu(II) ions bridged by two chloride ligands. On the basis of spectroscopic similarities (vide infra), an analogous structure is likely for the complex supported by $Ph(H_2L^{iPr2})^-$. These structures are distinct from those reported previously for the compounds supported by $H(Me_2L^{iPr2})^-$ and $Cl(Me_2L^{iPr2})^-$, both of which are mononuclear with 3-coordinate Cu(II) centers.[7a,d] Consistent with their higher coordination numbers, the metal−ligand bond distances in the dinuclear complexes are longer than those in the mononuclear species (average Cu−Cl = 2.32 Å vs 2.12 Å, Cu−N = 1.93 Å vs 1.87 Å). The coordination geometries of the metal ions in the dicopper complexes are distorted from tetragonal toward tetrahedral, as indicated by N−Cu−N/Cl−Cu−Cl dihedral angles of 51.78(4)° for $[Cl(Me_2L^{Me2})CuCl]_2$ and 50.05(7)° for $[H(Me_2L^{Et2})CuCl]_2$.[19] Such values that are intermediate between those of the tetragonal and tetrahedral extremes (0 and 90°, respectively) have been reported for other Cu(II) systems.[20] Although similar in most respects, the structures of the dicopper compounds differ from each other with respect to the relative

Scheme 1

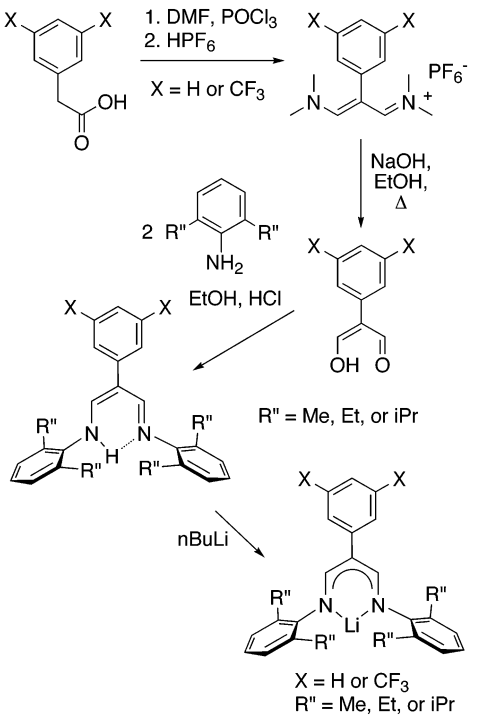

(10) A surprisingly stable neutral bis(μ-oxo)dicopper complex supported by an anionic iminophosphinamide ligand has been reported: Straub, B. F.; Rominger, F.; Hofmann, P. *Chem. Commun.* **2000**, 1611−1612.
(11) Dai, X.; Warren, T. H. *Chem. Commun.* **2001**, 1998−1999.
(12) Yokota, S.; Tachi, Y.; Nishiwaki, N.; Ariga, M.; Itoh, S. *Inorg. Chem.* **2001**, *40*, 5316−5317.
(13) Yokota, S.; Tachi, Y.; Itoh, S. *Inorg. Chem.* **2002**, *41*, 1342−1344.
(14) Cheng, M.; Moore, D. R.; Reczek, J. J.; Chamberlain, B. M.; Lobkovsky, E. B.; Coates, G. W. *J. Am. Chem. Soc.* **2001**, *123*, 8738−8749.
(15) For example, see: (a) Clegg, W.; Cope, E. K.; Edwards, A. J.; Mair, F. S. *Inorg. Chem.* **1998**, *37*, 2317−2319 and references therein. (b) Stender, M.; Wright, R. J.; Eichler, B. E.; Prust, J.; Olmstead, M. M.; Roesky, H. W.; Power, P. P. *J. Chem. Soc., Dalton Trans.* **2001**, 3465−3469 and references therein.
(16) The procedure used was adapted from one kindly provided to us by R. F. Jordan, University of Chicago.
(17) Davies, I. W.; Marcoux, J.-F.; Wu, J.; Palucki, M.; Corley, E. G.; Robbins, M. A.; Tsou, N.; Ball, R. G.; Dormer, P.; Larsen, R. D.; Reider, P. J. *J. Org. Chem.* **2000**, *65*, 4571−4574.
(18) So, J.-H.; Boudjouk, P. *Inorg. Chem.* **1990**, *29*, 1592−1593.
(19) This value for $[H(Me_2L^{Et2})CuCl]_2$ corresponds to the major (85%) component of the disordered structure. The value for the minor component is 51.75(17)°. For details, see the Experimental Section and the Supporting Information (CIF file).
(20) For example, see: Knapp, S.; Keenan, T. P.; Zhang, X.; Fikar, R.; Potenza, J.; Schugar, H. J. *J. Am. Chem. Soc.* **1990**, *112*, 3452−3464.

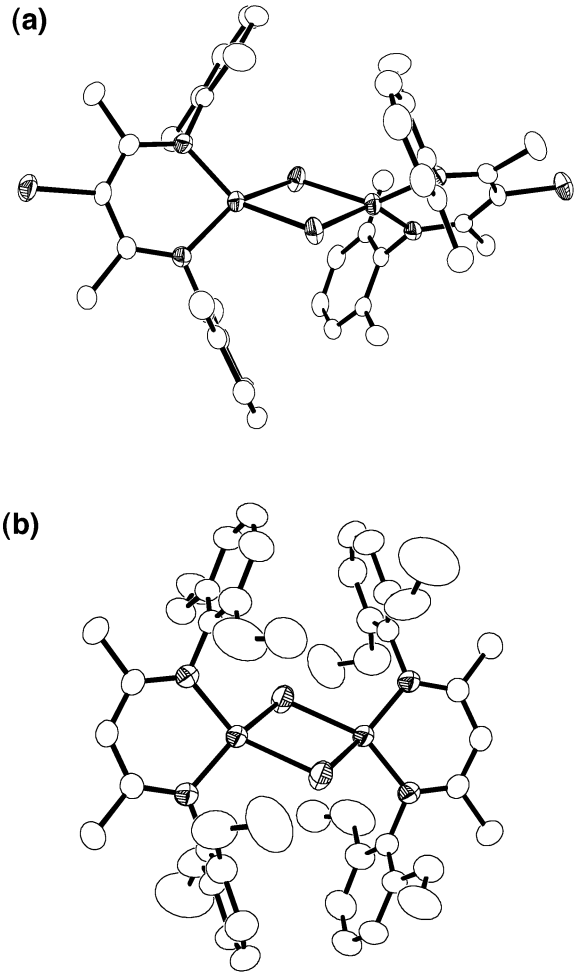

Figure 3. X-ray crystal structure representations of (a) $[Cl(Me_2L^{Me2})CuCl]_2$ and (b) $[H(Me_2L^{Et2})CuCl]_2$. All atoms are shown as (a) 50% or (b) 35% thermal ellipsoids with only heteroatoms labeled and hydrogen atoms omitted for clarity.

orientations of their β-diketiminates, as seen most readily by comparing the views down their respective Cu−Cu vectors (Figure 4). In $[H(Me_2L^{Et2})CuCl]_2$, the β-diketiminate N donors are "eclipsed" (Figure 4b), whereas in $[Cl(Me_2L^{Me2})CuCl]_2$ they are "staggered" (Figure 4a). Observation of the latter conformation is perhaps most significant, for it illustrates how interligand repulsions (i.e., between the aryl rings) may be alleviated in β-diketiminate-supported dicopper complexes that contain single-atom bridges.

In one case, $[Cl(Me_2L^{Me2})CuCl]_2$, the resultant magnetic moment as a function of temperature (5−300 K) and applied magnetic field (0.5−5 T) was measured for a powder sample using a SQUID magnetometer (Figure S1, Supporting Information). The data indicate only very weak antiferromagnetic coupling between the Cu(II) ions, with a fit to the 0.5 T data using the Van-Vleck formula (as described in the Experimental Section) yielding $J = -0.3(1)$ cm^{-1}, $g = 2.04(1)$, and $t = 5(1) \times 10^{-5}$ cm^3 mol^{-1}. The X-band EPR spectrum of a frozen solution of the complex in toluene at 20 K is shown in Figure 5a. Signals centered at $g = 4.9$, 2.5, 1.8, and 1.5 dominate the spectrum. The observation of such signals is consistent with the small J value and population of an $S = 1$ state at 20 K. We successfully simulated the features between 2000 and 4500 G (dotted line overlay in Figure 5a) using parameters for an $S = 1$ system with $g_1 = 2.11(1)$, $g_2 = 2.15(1)$, $g_3 = 2.16(2)$, $D = 0.156(1)$ cm^{-1}, and $E = 3(7) \times 10^{-4}$ cm^{-1} (line widths $W_x = 23(2)$ mT, $W_y = 10.5(5)$ mT, $W_z = 21(3)$ mT). The low-field signal ($g = 4.9$) corresponds to a $\Delta M_S = \pm 2$ transition, which was not simulated.[21] The EPR data are consistent with the retention in solution of the bis(μ-chloro)dicopper(II,II) structure determined by X-ray crystallography. In addition, a small amount (ca. 10% by integration) of a monomeric Cu(II) species in solution is indicated by the weak signal at $g \approx 2$ (presumably $Cl(Me_2L^{Me2})CuCl$; vide infra).

EPR spectra of toluene solutions of $[Ph(H_2L^{iPr2})CuCl]_2$ (Figure 5b) and $[H(Me_2L^{Et2})CuCl]_2$ (Figure 5c) also contain signals attributable to dinuclear species (cf. the low-field $\Delta M_S = \pm 2$ features), but with additional features at $g \approx 2.0$. In the spectrum of the latter complex the signal is axial with $g_{||} = 2.20$, $g_\perp = 2.05$, and $A^{Cu}_{||} = 128 \times 10^{-4}$ cm^{-1}. These parameters and, in particular, the signature low $A^{Cu}_{||}$ value, closely match those previously measured for the monomeric complexes LCuCl ($L = H(Me_2L^{iPr2})^-$ or $Cl(Me_2L^{iPr2})^-$).[7a,d] For example, the spectrum of $H(Me_2L^{iPr2})CuCl$ is characterized by $g_{||} = 2.20$, $g_\perp = 2.05$, and $A^{Cu}_{||} = 130 \times 10^{-4}$ cm^{-1}. Evidently, $[H(Me_2L^{Et2})CuCl]_2$ exists to a significant extent as $H(Me_2L^{Et2})CuCl$ at low temperature in toluene solution, suggesting the existence of an equilibrium between mono- and dinuclear forms of this complex (Scheme 2).

Support for this notion was provided by UV−vis data that were obtained over a range of temperatures for the chloro-bridged complexes. For example, solid samples of $[H(Me_2L^{Et2})CuCl]_2$ are green, yet solutions in toluene or CH_2Cl_2 are deep purple. UV−vis spectra of these purple solutions (Figure 6a) are invariant over $-50\ ^\circ C < T < 25\ ^\circ C$ and are essentially identical to that of the monomeric 3-coordinate complexes supported by $H(Me_2L^{iPr2})^-$ or $Cl(Me_2L^{iPr2})^-$ (cf. dashed line in Figure 6a).[7a,d] These data show that while dinuclear as a solid, $[H(Me_2L^{Et2})CuCl]_2$ dissociates essentially entirely upon dissolution to $H(Me_2L^{Et2})CuCl$ under these conditions, with the EPR data (Figure 5c) showing the presence of both mono- and dinuclear forms in solution at lower temperatures (20 K). The relative stabilities of the mono- and dinuclear forms are shifted for the systems supported by $Ph(H_2L^{iPr2})^-$ and $Cl(Me_2L^{Me2})^-$, as indicated by temperature-dependent UV−vis spectra, exemplified for the latter case in Figure 6b. At 22.5 °C, only spectral features diagnostic for the 3-coordinate monomer are evident (dotted line), but at −55.0 °C the spectrum is significantly different, with new bands at ~480 and ~690 nm (solid line). Intermediate spectra were obtained at temperatures between these extremes, and the spectral changes were fully reversible. These data are consistent with the presence of an equilibrium between $[Cl(Me_2L^{Me2})CuCl]_2$ and $Cl(Me_2L^{Me2})CuCl$, the dinuclear species with features at 480 and 690 nm being favored at lower temperatures. Similar data that support the same conclusion were obtained for $[Ph(H_2L^{iPr2})CuCl]_2$ (Figure S2).[9a]

(21) Pilbrow, J. R. *Transition Ion Electron Paramagnetic Resonance*; Clarendon Press: Oxford, U.K., 1990; Chapter 7.

Table 1. Summary of X-ray Crystallographic Data

	[Ph(H$_2$L^{iPr2})Cu(MeCN)][a]	[3,5-(CF$_3$)$_2$C$_6$H$_3$(H$_2$L^{iPr2})Cu(MeCN)][a]	[H(Me$_2$L^{Me2})Cu(CNC$_6$H$_3$Me$_2$)][a]
empirical formula	$C_{35}H_{44}CuN_3$	$C_{37}H_{44}CuF_6N_3$	$C_{30}H_{33}ClCuN_3$
fw	570.27	706.28	534.58
cryst system	monoclinic	triclinic	monoclinic
space group	Cc	$P\bar{1}$	$P2_1/c$
a (Å)	9.927(3)	9.4815(18)	11.7422(18)
b (Å)	20.216(5)	13.068(3)	11.4347(6)
c (Å)	16.489(5)	14.499(3)	20.519(3)
α (deg)	90	96.998(3)	90
β (deg)	96.031(4)	95.087(3)	97.356(7)
γ (deg)	90	94.424(3)	90
V (Å^3)	3290.8(16)	1769.0(6)	2732.4(6)
Z	4	2	4
D_{calc} (g cm^{-3})	1.151	1.326	1.299
cryst dimens	1.33 × 0.63 × 0.15	0.20 × 0.15 × 0.15	0.25 × 0.25 × 0.15
θ range (deg)	2.01−25.03	1.42−25.07	1.75−25.05
abs coeff (mm^{-1})	0.689	0.678	0.920
reflcns collcd	22 831	12 604	13 114
unique reflcns	5548	6219	4814
params	372	467	324
R1, wR2 (for $I > 2\sigma(I)$)[c]	0.0381, 0.1010	0.0558, 0.1424	0.0374, 0.0885
goodness-of-fit	0.988	1.046	1.007
largest peak, hole (e/Å^{-3})	0.606, −0.341	0.411, −0.587	0.478, −0.426

	[Cl(Me$_2$L^{Me2})CuCl]$_2$[a]	[H(Me$_2$L^{Et2})CuCl]$_2$[b]	[NO$_2$(H$_2$L^{Me2Me})Cu(OH)$_2$][b]
empirical formula	$C_{42}H_{48}Cu_2Cl_4N_4$	$C_{50}H_{66}Cu_2N_4Cl_2$	$C_{42}H_{50}Cu_2N_6O_6$
fw	877.72	921.05	861.99
cryst system	monoclinic	monoclinic	orthorhombic
space group	*C*2/*c*	$P2_1/n$	Pbcn
a (Å)	18.9825 (5)	13.6615 (9)	21.4089(6)
b (Å)	11.6252 (2)	12.5107 (8)	8.0931(2)
c (Å)	20.3111 (5)	15.1162 (10)	24.2109(7)
α (deg)	90	90	90
β (deg)	114.6590 (10)	109.2870 (10)	90
γ (deg)	90	90	90
V (Å^3)	4073.42 (16)	2438.6 (3)	4194.9(2)
Z	4	2	4
D_{calc} (g cm^{-3})	1.431	1.254	1.365
cryst dimens	0.4 × 0.4 × 0.15	0.5 × 0.4 × 0.3	0.5 × 0.2 × 0.2
θ range (deg)	2.11−24.97	2.38−25.04	2.1−27.5
abs coeff (mm^{-1})	1.342	1.018	1.067
reflcns collcd	10 141	18 235	9618
unique reflcns	3576	4299	3128
params	241	284	279
R1, wR2 (for $I > 2\sigma(I)$)[c]	0.0242, 0.0637	0.0339, 0.0980	0.0340, 0.0450
goodness-of-fit	1.033	0.997	1.025
largest peak, hole (e/Å^{-3})	0.263, −0.362	0.356, −0.230	0.40, −0.42

[a] Structures determined at $T = -100$ °C. [b] Structures determined at $T = +20$ °C. [c] $R1 = \Sigma||F_o| - |F_c||/|F_o|$; $wR2 = [\Sigma w(F_o^2 - F_c^2)^2/\Sigma w(F_o^2)^2]^{1/2}$, where $w = 1/[\sigma^2(F_o^2 + (aP)^2 + bP]$, $P = (F_o^2 + 2F_c^2)/3$, and *a* and *b* are constants given in the Supporting Information.

Taken together, the structural and spectroscopic results reported previously[7,9a] and described herein for the series $[LCuCl]_n$ ($n = 1$ or 2, L = *β*-diketiminate) provide important experimental measures of the steric influences of the supporting ligands. Those ligands with backbone α-substituents and aryl ^{i}Pr groups (e.g., H(Me$_2$L^{iPr2})$^-$, Cl(Me$_2$L^{iPr2})$^-$, and H(tBu$_2$L^{iPr2})$^-$) are sufficiently encumbered to prevent dimerization and to yield only monomeric 3-coordinate species LCuCl ($n = 1$). Ligands with either smaller aryl groups or which lack backbone α-substituents (e.g., H(Me$_2$L^{Et2})$^-$, Cl(Me$_2$L^{Me2})$^-$, and Ph(H$_2$L^{iPr2})$^-$) yield complexes that are dinuclear ($n = 2$) in the solid state and at low temperature in solution but which are prone to dissociation to monomeric species in solution at higher temperatures. These *β*-diketiminate ligand steric differences that are the basis for the structural variances in the compounds $[LCuCl]_n$ also underly differences in the structures and O_2 reactivity of Cu(I) complexes, as discussed below.

Syntheses and Structures of Cu(I) Complexes. With only a few exceptions, reaction of the lithium *β*-diketiminates with $[Cu(MeCN)_4]CF_3SO_3$ in THF yielded Cu(I) complexes of the general formula LCu(MeCN) that were isolated as yellow solids (Scheme 3). One exception was [NO$_2$(H$_2$L^{Me2Me})-Cu(MeCN)], which was synthesized in situ by the addition of MeCN to $[NO_2(H_2L^{Me2Me})Cu]_n$.[12] In the case of Cl-(Me$_2$L^{Me2})H, reaction of its lithium salt with $[Cu(MeCN)_4]$-CF_3SO_3 invariably resulted in disproportionation, as evidenced by coloration of the reaction solution (dark brown) and the appearance of a dark red precipitate. The only route to a Cu(I) complex of this ligand that we have found so far involves treating Cl(Me$_2$L^{Me2})H with $[CuCH_2SiMe_3]_4$[22] in the presence of an aryl isocyanide "trap", $CNC_6H_3Me_2$, to yield

(22) (a) Lappert, M. F.; Pearce, R. *Chem. Commun.* **1973**, 24−25. (b) Jarvis, J. A.; Kilbourn, B. T.; Pearce, R.; Lappert, M. F. *Chem. Commun.* **1973**, 475−476. (c) Jarvis, J. A. J.; Pearce, R.; Lappert, M. F. *J. Chem. Soc., Dalton Trans.* **1977**, 999−1003.

Table 2. Selected Interatomic Distances (Å) and Angles (deg)[a]

	[Ph(H_2L^{iPr2})Cu(MeCN)]		
Cu−N1	1.964(2)	Cu1−N5	1.950(2)
Cu−N1S	1.860(3)	N5−Cu1−N1	97.25(9)
N1−Cu1−N1S	128.19(11)	N5−Cu1−N1S	133.75(10)
	[3,5-$(CF_3)_2C_6H_3$(H_2L^{iPr2})Cu(MeCN)]		
Cu1−N1	1.908(3)	Cu1−N5	1.977(3)
Cu1−N1S	1.862(4)	Cu1−N1S	1.977(17)
N1−Cu1−N5	97.59(11)	N1−Cu1−N1S	155.09(15)
N5−Cu1−N1S	106.86(15)	N1−Cu1−N1S	101.4(5)
N5−Cu1−N1S	152.9(5)	N1S−Cu1−N1S	57.7(5)
	[Cl(Me_2L^{Me2})Cu($CNC_6H_3Me_2$)]		
Cu1−N1	1.931(2)	Cu1−N2	1.954(2)
Cu1−C22	1.824(3)	N1−Cu1−N2	95.51(8)
N1−Cu1−C22	137.64(10)	N2−Cu1−C22	126.84(10)
Cu1−C22−N3	176.0(2)		
	[Cl(Me_2L^{Me2})CuCl]$_2$		
Cu1−N1	1.9223(15)	Cu1−N2	1.9194(15)
Cu1−Cl1	2.3319(5)	Cu1−Cl1′	2.3092(5)
Cu1−Cu1′	3.3763(4)	N2−Cu1−Cl1	100.47(5)
N1−Cu1−N2	94.67(6)	N1−Cu1−Cl1′	100.39(5)
N1−Cu1−Cl1	143.58(5)	N2−Cu1−Cl1′	143.67(5)
		Cl1−Cu1−Cl1′	86.631(18)
	[H(Me_2L^{Et2})CuCl]$_2$		
Cu1−N1	1.9297(18)	Cu1−N2	1.9295(19)
Cu1−Cl1	2.3274(7)	Cu1−Cl1′	2.3194(7)
Cu1−Cu1′	3.4243(5)	N1−Cu1−N2	95.59(8)
N1−Cu1−Cl1	146.02(7)	N1−Cu1−Cl1′	100.83(6)
N2−Cu1−Cl1	99.12(6)	N2−Cu1−Cl1′	143.48(7)
Cl1−Cu1−Cl1′	85.06(3)	Cl1−Cu1−Cl1′	85.06(3)
	[NO_2(H_2L^{Me2Me})Cu(μ-OH)$_2$]		
Cu1−O3	1.905(2)	Cu1−N1	1.940(2)
Cu1−N2	1.934(2)	Cu1−Cu1′	3.005(1)
O3−O3′	2.341(4)	O3−Cu1−N1	96.7(1)
O3−Cu1−N2	163.27(11)	N1−Cu1−N2	94.3(1)

[a] Estimated standard deviations in parentheses. "S" refers to atoms of bound solvent molecules, and prime symbols refer to symmetry-related atoms (see CIF for details).

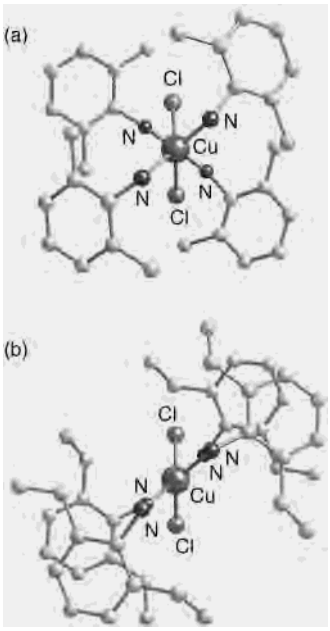

Figure 4. Views along the Cu−Cu vectors of the X-ray structures of (a) [Cl(Me_2L^{Me2})CuCl]$_2$ and (b) [H(Me_2L^{Et2})CuCl]$_2$. The β-diketiminate backbone and backbone substituent atoms have been omitted for clarity.

[Cl(Me_2L^{Me2})Cu($CNC_6H_3Me_2$)], which was isolated as a light yellow crystalline solid. This compound and the other

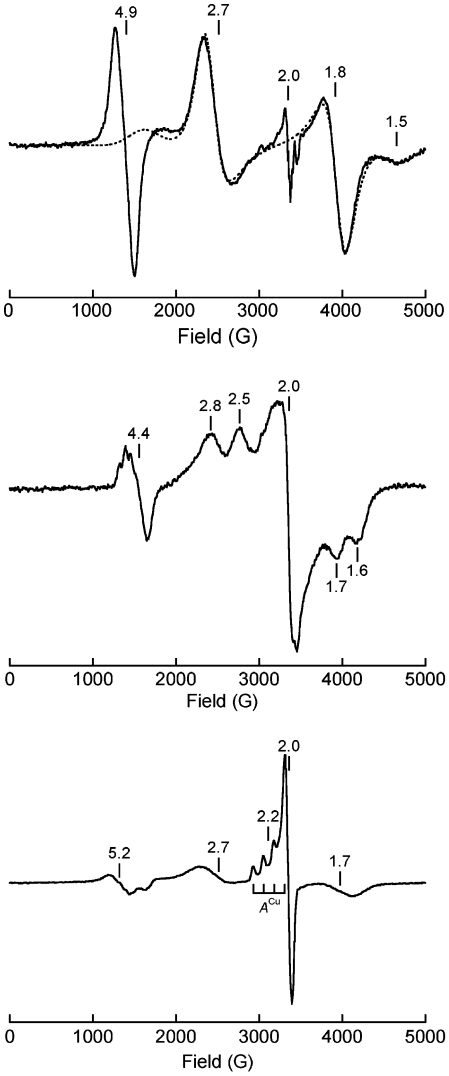

Figure 5. EPR spectra of (a) [Cl(Me_2L^{Me2})CuCl]$_n$ in toluene, 9.600 GHz, 20 K, with simulation overlaid as dotted line (see text for parameters), (b) [Ph(H_2L^{iPr2})CuCl]$_n$ in toluene, 9.614 GHz, 20 K, and (c) [H(Me_2L^{Et2})CuCl]$_n$ in toluene, 9.590 GHz, 4 K. The annotations are approximate g values obtained from inspection.

Scheme 2

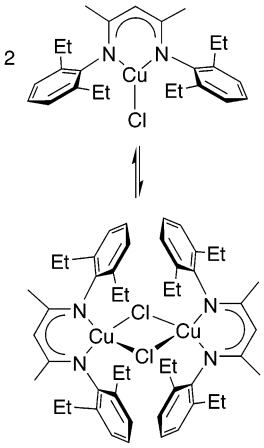

isolable Cu(I) complexes were characterized by ^{1}H NMR and UV−vis spectroscopy, elemental analysis, and, in three instances, by X-ray crystallography. In general, the spectral data are unremarkable and are consistent with the formulated

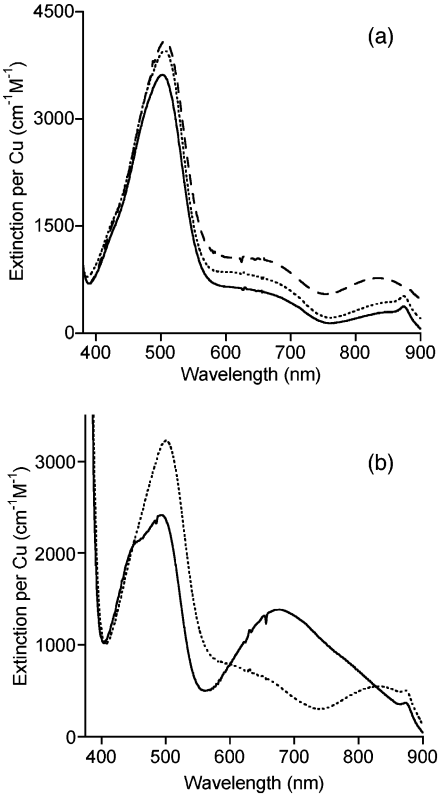

Figure 6. (a) UV−vis spectra of $[H(Me_2L^{Et2})CuCl]_n$ in toluene at 22.4 °C (—) and −49.8 °C (···), overlaid with the spectrum of $H(Me_2L^{iPr2})CuCl$ in CH_2Cl_2 (- − -).[7a] (b) UV−vis spectra of $[Cl(Me_2L^{Me2})CuCl]_2$ in toluene at 22.4 °C (···) and −55.0 °C (—).

structures, but it is worth noting that those complexes that contain a central methine β-diketiminate backbone substituent (R) exhibit an intense electronic absorption feature that is sensitive to the nature of the R group (Table 3). Thus, an absorption band at $\lambda_{max} \approx 380$ nm ($\epsilon \approx 20\,000$ M^{-1} cm^{-1}/Cu) for the compounds with R = Ph appears at ∼15 nm longer wavelength than for the complexes with R = 3,5-$(CF_3)_2C_6H_3$. The energy, intensity, and sensitivity of this feature to the electron-withdrawing capability of the R group are consistent with an assignment as a β-diketiminate ligand-based $\pi \rightarrow \pi^*$ transition.[7c]

Representations of the X-ray crystal structures of $[Ph(H_2L^{iPr2})Cu(MeCN)]$, $[3,5\text{-}(CF_3)_2C_6H_3(H_2L^{iPr2})Cu(MeCN)]$, and $[Cl(Me_2L^{Me2})Cu(CNC_6H_3Me_2)]$ are shown in Figure 7, with selected crystallographic data and interatomic distances and angles listed in Tables 1 and 2, respectively. The Cu(I) centers generally exhibit 3-coordinate, planar, approximately C_{2v}-symmetric geometries, as indicated by sums of N−Cu−N angles equal to 360 ± 1° and approximately equal N−Cu−N_{MeCN} or N−Cu−C angles (Δ values ≤ 11°).[23] The one exception is $[3,5\text{-}(CF_3)_2C_6H_3(H_2L^{iPr2})Cu(MeCN)]$, in which the MeCN ligand is disordered over two positions (84:16 ratio) characterized by large Δ values (48 and 52°), resulting in a site symmetry significantly distorted from C_{2v}. The average Cu−N(β-diketiminate) bond distance among the three compounds is 1.95 Å, within the range of analogous

Scheme 3

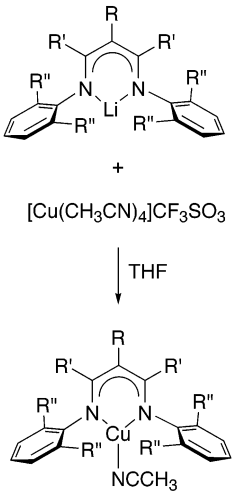

distances in other Cu(I)−β-diketiminate complexes (1.90−1.99 Å)[7d,9,11,12] but longer than in 3-coordinate Cu(II)−β-diketiminate species (1.86−1.90 Å) as expected on the basis of the metal oxidation level.[7] The structures are generally similar to previously reported analogues supported by the more sterically encumbered ligands $H(Me_2L^{iPr2})^-$ or $H(tBu_2L^{iPr2})^-$,[9] but there is a noteworthy difference involving the orientation of the ^{i}Pr groups. In $[H(Me_2L^{iPr2})Cu(MeCN)]$, the ^{i}Pr group methine hydrogen atoms point inward toward the β-diketiminate ligand in an orientation typical for complexes of $H(Me_2L^{iPr2})^-$.[6−9] Steric interactions between the backbone methyl and the ^{i}Pr groups presumably are responsible for this conformational preference. In contrast, in $[Ph(H_2L^{iPr2})Cu(MeCN)]$ and $[3,5\text{-}(CF_3)_2C_6H_3(H_2L^{iPr2})Cu(MeCN)]$ that lack the β-diketiminate backbone methyl groups, one or more of the ^{i}Pr groups are rotated away from this orientation by up to 180° (cf. bottom left ^{i}Pr group in Figure 7a). Recognizing the possible impact of ill-defined crystal packing forces, we nonetheless hypothesize that the presence of these alternate rotomers indicates greater ^{i}Pr group conformational flexibility that results in decreased effective steric bulk in these systems relative to those that contain an α-alkyl group, such as $H(Me_2L^{iPr2})^-$. These notions are further supported by the reactivity results described below.

Electrochemistry of Cu(I) Complexes. Cyclic voltammetry experiments were performed on solutions of the Cu(I) complexes in MeCN with 0.1 M Bu_4NPF_6 at room temperature. All the compounds exhibit a reversible anodic wave when scanned initially to either reductive or oxidative potential, with $i_a \approx i_b$ and values of $E_{pa} - E_{pc}$ in the range 78−110 mV that do not vary as a function of scan rate between 100 and 350 mV s^{-1} (cf. Figure S3). We attribute this wave to the Cu(I)/Cu(II) redox couple. The values for $E_{1/2}$ (vs NHE)[24] are listed in Table 4.[25] The low potentials reflect the strong electron-donating capability of the β-diketiminate ligands;[7c] by comparison, potentials reported for other

(23) Δ = the difference between the N−Cu−N_{MeCN} or N−Cu−C angles. For example, for $[Ph(H_2L^{iPr2})Cu(MeCN)]$, Δ = |(∠N1−Cu1−N1S) − (∠N5−Cu1−N1S)| = |128.19(11)° − 133.75(10)°| = 5.6°.

(24) The values vs NHE were obtained by adding 640 mV to the value measured versus Fc/Fc^+ in CH_3CN with Bu_4NPF_6 as electrolyte, according to Table 1 in the following: Connelly, N. G.; Geiger, W. E. *Chem. Rev.* **1996**, *96*, 877−910.

(25) In the cathodic region each complex exhibited an irreversible reduction.

Table 3. Spectroscopic Properties of Cu(I) Complexes and Derived Bis(μ-oxo)dicopper Intermediates[a]

ligand	UV−vis λ_{max} (nm) (ϵ, M^{-1} cm^{-1}) of Cu(I) complex	UV−vis λ_{max} (nm) (ϵ, M^{-1} cm^{-1}) of intermediate	resonance Raman $\nu(Cu_2O_2)$ (cm^{-1}) of intermediate
$H(Me_2L^{Et2})$	348 (27 000)	426 (10 000),[b] 352 (22 000), 332 (sh, 27 000)	604 (577)
$H(Me_2L^{Me2})$	340 (20 000)	422 (11 000),[b] 344 (sh, 32 000), 328 (37 000)	608 (581)
$Ph(H_2L^{iPr2})$	378 (21 000), 298 (36 000)	433 (sh, 7600),[b] 369 (20 000)	580 (560)
$Ph(H_2L^{Et2})$	381 (21 000), 298 (36 000)	425 (16 500),[b] 379 (20 000)	591/617 (574)
$Ph(H_2L^{Me2})$	378 (19 000), 298 (25 000)	420 (12 200),[b] 377 (19 000)	586/614 (573)
$3,5\text{-}(CF_3)_2C_6H_3(H_2L^{iPr2})$	365 (sh, 19 000), 328 (31 000)	433 (15 500),[b] 360 (sh, 21 000), 312 (35 000)	574/581 (563)
$3,5\text{-}(CF_3)_2C_6H_3(H_2L^{Et2})$	366 (sh, 19 000), 328 (34 000)	423 (13 200),[b] 361 (sh, 18 000), 318 (26 000)	592/607/613 (573)
$3,5\text{-}(CF_3)_2C_6H_3(H_2L^{Me2})$	365 (sh, 21 000), 331 (26 000)	417 (19 700),[b] 361 (sh, 21 000), 317 (29 000)	586/618 (575)
$3,5\text{-}(CF_3)_2C_6H_3(H_2L^{CH3,CD3})$	366 (sh, 20 000), 324 (36 000)	416 (16 200),[b] 361 (sh, 20 000), 314 (35 000)	580/617 (573)
$NO_2(H_2L^{Me2Me})$	381 (24 600)[c]	440 ($\approx$17 800)[b,c]	599/624 (582)[d]

[a] Except as noted, all UV−vis and Raman spectra were measured in THF, with extinction coefficents reported per Cu. Except as noted, UV−vis spectra of the oxygenated intermediates were obtained at −80 °C and resonance Raman spectra were obtained at −196 °C using 457.9 nm laser excitation. Only ^{18}O-sensitive vibrations in Raman spectra are quoted with data acquired using $^{18}O_2$ listed in parentheses. [b] This extinction coefficient reported per bis(μ-oxo)dicopper complex to facilitate comparison to literature values. [c] Measured in MeCN at −40 °C. [d] Data obtained at −196 °C on MeCN solutions.

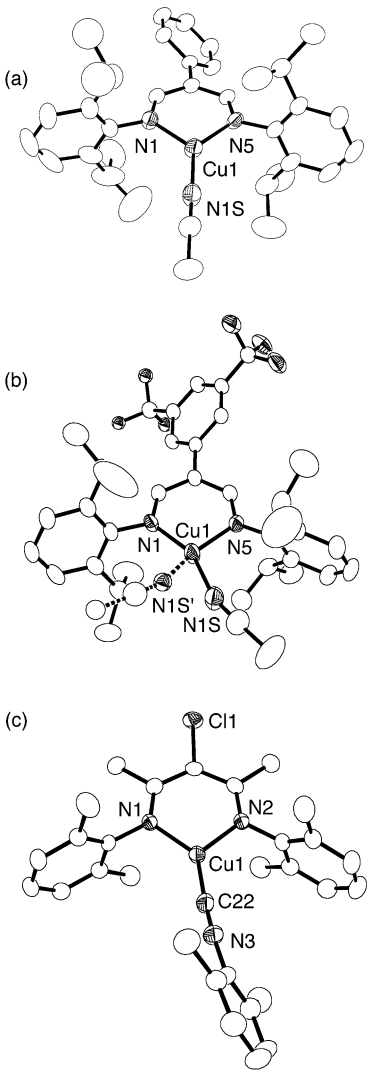

Figure 7. X-ray crystal structure representations of (a) [$Ph(H_2L^{iPr2})$Cu(MeCN)], (b) [$3,5\text{-}(CF_3)_2C_6H_3(H_2L^{iPr2})$Cu(MeCN)], and (c) [$Cl(Me_2L^{Me2})$-$Cu(CNC_6H_3Me_2)$]. All atoms are shown as 50% thermal ellipsoids with only heteroatoms labeled (except for the fluorine atoms in (b)), and hydrogen atoms are omitted for clarity.

three coordinate Cu(I) complexes with neutral N-donors and MeCN ligands are significantly more positive (by ca. +0.5 V).[26] Additional anionic coligands depress the $E_{1/2}$ values further, as reflected by the data for Cu(II)/Cu(I) couples

Table 4. Values of $E_{1/2}$ for β-Diketiminate−Copper Complexes

entry	complex	$E_{1/2}$ (mV)[d]	ΔE_P (mV)[d]	ref
1	$[H(Me_2L^{iPr2})Cu(MeCN)]$[a]	+425	95	this work
2	$[H(Me_2L^{Et2})Cu(MeCN)]$[a]	+343	84	this work
3	$[H(Me_2L^{Me2})Cu(MeCN)]$[a,b]	+309	74	this work
4	$[Ph(H_2L^{iPr2})Cu(MeCN)]$[a]	+384	105	this work
5	$[Ph(H_2L^{Et2})Cu(MeCN)]$[a]	+420	100	this work
6	$[Ph(H_2L^{Me2})Cu(MeCN)]$[a]	+388	100	this work
7	$[3,5\text{-}(CF_3)_2C_6H_3(H_2L^{iPr2})Cu(MeCN)]$[a]	+449	110	this work
8	$[3,5\text{-}(CF_3)_2C_6H_3(H_2L^{Et2})Cu(MeCN)]$[a]	+428	95	this work
9	$[3,5\text{-}(CF_3)_2C_6H_3(H_2L^{Me2})Cu(MeCN)]$[a]	+400	106	this work
10	$[NO_2(H_2L^{Me2Me})Cu(MeCN)]$[a]	+520	78	this work
11	$[H(Me_2L^{iPr2})CuCl]$[c]	−80	70	7a
12	$[H(Me_2L^{iPr2})CuSCPh_3]$[c]	−180	80	7a
13	$[H(Me_2L^{iPr2})CuOC_6H_4{}^tBu]$[c]	−260	79	7d
14	$[H(Me_2L^{iPr2})CuOC_6H_4OMe]$[c]	−280	76	7d

[a] All values reported vs NHE, by adding 640 mV to the value measured vs the ferrocene/ferrocenium couple in CH_3CN (+0.642 V vs Ag wire) with Bu_4NPF_6 as electrolyte.[19] [b] For this compound, the $E_{1/2}$ value shifted over multiple runs, a degree of irreproducibility that suggests that the redox process may be more complex than for the other systems. [c] Measured in THF with Bu_4NPF_6 as electrolyte, cited vs NHE. [d] Measurements at a scan rate of 100 mV s^{-1}.

measured for a range of β-diketiminate Cu(II) halide, phenoxide, and thiolate complexes (entries 11−14).[7] Effects of β-diketiminate ligand substituent variation in otherwise alike compounds are apparent, but they are generally small. For example, comparison of the data in entries 4 and 7 for complexes with ligands that are identical except for the central β-diketiminate backbone substituent (Ph vs $3,5\text{-}(CF_3)_2C_6H_3$) reveals a shift of +65 mV as the electron-withdrawing capability of the substituent increases. Decreased shifts for the same backbone substituent comparison are observed when the R″ groups are smaller (e.g., +8 mV for entries 5 and 8, +12 mV for entries 6 and 9). Finally, the influence of the nitro group is most significant, as the potential for $[NO_2(H_2L^{Me2Me})Cu(MeCN)]$ (entry 10) is $\approx$100 mV more anodic than for the other Cu(I) complexes. All of these potential shifts are consistent with decreased stabilization of the Cu(II) state relative to the Cu(I) state as the strong electron donation by the β-diketiminate is modulated by electron withdrawing substituents. Importantly, however, the differences in $E_{1/2}$ values among the Cu(I) compounds listed

(26) Yates, P. C.; Drew, M. G. B.; Trocha-Grimshaw, J.; McKillop, K. P.; Nelson, S. M.; Ndifon, P. T.; McAuliffe, C. A.; Nelson, J. *J. Chem. Soc., Dalton Trans.* **1991**, 1973−1979.

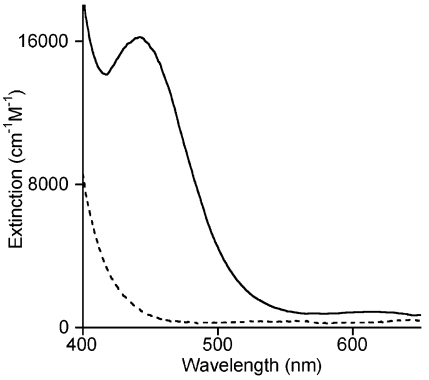

Figure 8. UV−vis absorption spectra of THF solutions at −80 °C of [3,5-$(CF_3)_2C_6H_3(H_2L^{iPr})$Cu(MeCN)] (···) and the product of its oxygenation (−). The extinction coefficient (*y* axes) for the product are per bis(μ-oxo)-dicopper complex.

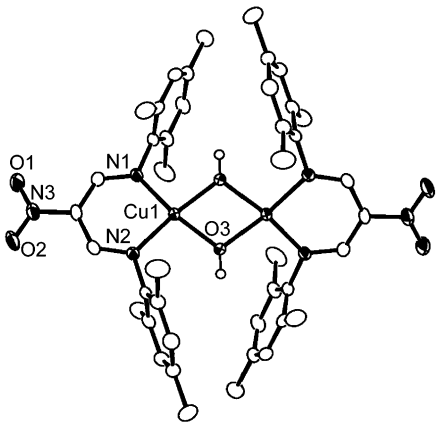

Figure 9. X-ray crystal structure representation of [{$NO_2(H_2L^{Me2Me})$Cu}$_2$-(μ-OH)$_2$]. All atoms are shown as 50% thermal ellipsoids with only heteroatoms labeled and hydrogen atoms and solvent molecules omitted for clarity (except for the hydrogen atoms on the hydroxo bridge).

in Table 4 do not correlate with differences in the course of their reactions with O_2 (vide infra).

Dioxygen Reactivity. The Cu(I) complexes prepared in this work are exceedingly air sensitive. Treatment of solutions of the complexes in THF with O_2 at −80 °C induced a color change to golden-brown or green; representative UV−vis spectral changes are shown in Figure 8. A similar reaction was observed upon oxygenation of [NO_2-(H_2L^{Me2Me})Cu(MeCN)] in MeCN at −40 °C. The oxygenated species were EPR silent (frozen solution, X-band, 2−20 K). Bubbling of argon through the intermediate solutions at low-temperature did not induce spectral changes, indicating that the oxygenation process is irreversible under the conditions used. Spectrophotometric titration data for the reaction of [Ph(H_2L^{iPr2})Cu(MeCN)] showed a Cu:O_2 stoichiometry of 2.0(2):1. In an alternate route, addition of 1−5 equiv of a 1:1 solution of H_2O_2(aq) (31.3%) and Et_3N to a solution of [Ph(H_2L^{iPr2})CuCl]$_n$ in THF or toluene at −40 °C yielded UV−vis spectral features similar to those seen upon oxygenation of [Ph(H_2L^{iPr2})Cu(MeCN)]. No reaction of the Cu(II) precursor with H_2O_2 was observed in the absence of NEt_3. All of the intermediate solutions changed color upon warming yet remained essentially EPR silent,[27] signifying conversion to a magnetically coupled dicopper(II,II) species. In one instance, with the ligand $NO_2(H_2L^{Me2Me})^-$, a bis(μ-hydroxo)dicopper(II,II) complex was isolated from the decomposed solution and was structurally characterized by X-ray crystallography (Figure 9). The β-diketiminates adopt an eclipsed conformation, similar to that of [H(Me_2L^{Et2})-CuCl]$_2$ (Figure 4b). In general, the structure is unexceptional, being rather similar to those of previously reported complexes of this type.[11,28]

The UV−vis spectra of the colored intermediate solutions contain intense bands at $\lambda_{max} \approx 380$ nm ($\epsilon \approx 20\,000$ M^{-1} cm^{-1}/Cu) and ≈ 425 nm ($\epsilon \approx 10\,000-20\,000$ M^{-1} cm^{-1}/dicopper complex), as well as a broad, weak band at $\lambda_{max} \approx 600$ nm ($\epsilon \approx 100$ M^{-1} cm^{-1}/Cu) (Figure 8 and Table 3). By analogy to the Cu(I) cases, we assign the intense high-energy feature as a β-diketiminate-based $\pi \rightarrow \pi^*$ transition. As observed for the Cu(I) complex precursors, this band is sensitive to the β-diketiminate R group and shifts to shorter wavelength as the electron-withdrawing capability of the R group is increased. As a result, the ≈420 nm band appears as a largely obscured shoulder when R = Ph and is more readily discerned for R = 3,5-$(CF_3)_2C_6H_3$ (Figure 8). The nature of the R group does not affect the ∼420 nm feature significantly, suggesting that this charge transfer band does not involve the β-diketiminate ligand in any significant way. Instead, the energy and intensity of this feature are reminiscent of those of a band with oxo → Cu(III) CT character that is firmly associated with bis(μ-oxo)dicopper complexes.[2e,3,29,30]

To corroborate this electronic absorption spectral assignment and the conclusion that the intermediates are indeed bis(μ-oxo)dicopper species, we collected resonance Raman spectra of frozen THF solutions using an excitation wavelength of 457.9 nm at −196 °C. Spectra were acquired on samples prepared with $^{16}O_2$ or $^{18}O_2$ to conclusively identify vibrational features involving incorporated oxygen atoms. Numerous resonance-enhanced features were observed, but only a few in the 550−625 cm^{-1} range were found to be O-isotope sensitive; these are listed in Table 3. Illustrative spectra of the intermediates derived from [3,5-$(CF_3)_2C_6H_3$-(H_2L^{Me2})Cu(MeCN)] and [Ph(H_2L^{iPr2})Cu(MeCN)] are shown in Figure 10, and plots of all spectra are presented in Figure S4.

For the system supported by $Ph(H_2L^{iPr2})^-$ (Figure 10b), a single peak appears at ∼580 cm^{-1} which shifts by −20 cm^{-1} when $^{18}O_2$ is used. We assign this feature as an A_g symmetry $[Cu_2(\mu\text{-}O)_2]^{2+}$ core vibration by analogy to published data on bis(μ-oxo)dicopper complexes.[2e,3,29] An identical spec-

(27) An axial signal from a monocopper(II) species was observed for the warmed solutions, but values for spin quantitation were only between 1 and 7% (versus an external standard).

(28) Mahapatra, S.; Halfen, J. A.; Wilkinson, E. C.; Pan, G.; Wang, X.; Young, V. G., Jr.; Cramer, C. J.; Que, L., Jr.; Tolman, W. B. *J. Am. Chem. Soc.* **1996**, *118*, 11555−11574.

(29) (a) Henson, M. J.; Mukherjee, P.; Root, D. E.; Stack, T. D. P.; Solomon, E. I. *J. Am. Chem. Soc.* **1999**, *121*, 10332−10345. (b) Holland, P. L.; Cramer, C. J.; Wilkinson, E. C.; Mahapatra, S.; Rodgers, K. R.; Itoh, S.; Taki, M.; Fukuzumi, S.; Que, L., Jr.; Tolman, W. B. *J. Am. Chem. Soc.* **2000**, *122*, 792−802.

(30) Mahadevan, V.; Hou, Z.; Cole, A. P.; Root, D. E.; Lal, T. K.; Solomon, E. I.; Stack, T. D. P. *J. Am. Chem. Soc.* **1997**, *119*, 11996−11997.

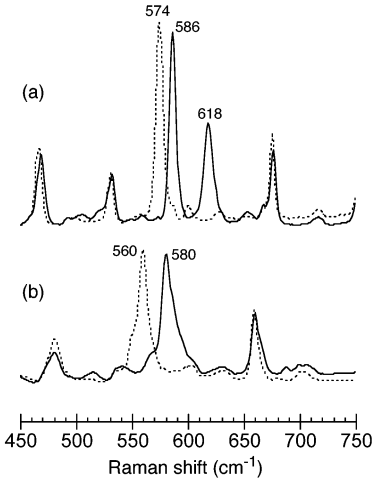

Figure 10. Resonance Raman spectra (λ_{ex} = 457.9 nm, −196 °C) of THF solutions of the intermediates resulting from the reactions of $^{16}O_2$ (—) or $^{18}O_2$ (···) with (a) [3,5-$(CF_3)_2C_6H_3$(H_2L^{Me2})Cu(MeCN)] and (b) [Ph(H_2L^{iPr2})-Cu(MeCN)].

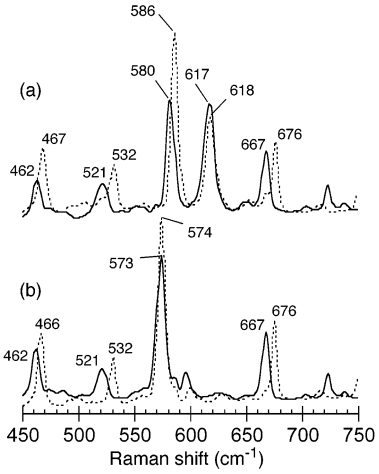

Figure 11. Resonance Raman spectra (λ_{ex} = 457.9 nm, −196 °C) of THF solutions of the intermediates resulting from the reactions of [3,5-$(CF_3)_2C_6H_3$($H_2L^{CH3,CD3}$)Cu(MeCN)] (—) and [3,5-$(CF_3)_2C_6H_3$(H_2L^{Me2})Cu-(MeCN)] (···) with (a) $^{16}O_2$ and (b) $^{18}O_2$.

trum was obtained for the solution resulting from mixing [Ph(H_2L^{iPr2})CuCl]$_x$ with H_2O_2/NEt_3, proving that the same bis(μ-oxo)dicopper complex formed in this alternative preparation. Single peaks also were observed for the systems supported by H(Me_2L^{Me2})$^-$ and H(Me_2L^{Et2})$^-$ (Table 3, Figure S4). For all other systems, two peaks of variable relative intensity are observed in the spectra of the $^{16}O_2$-derived intermediates, and these convert to a single peak when $^{18}O_2$ is used (cf. Figure 10a). With one exception, the difference between the average of the two $^{16}O_2$ bands and the single $^{18}O_2$ peak falls in the range 25−30 cm^{-1}. The exception is the system supported by 3,5-$(CF_3)_2C_6H_3$(H_2L^{iPr2})$^-$, for which the $^{16}O_2$ bands are barely resolved and the difference between the average and the $^{18}O_2$ peak is ∼15 cm^{-1} (Figure S4).

The observation of multiple bands for only one oxygen isotopomer ($^{16}O_2$) suggests some type of vibrational mixing of the [$Cu_2(\mu$-$O)_2$]$^{2+}$ core mode either with an overtone or combination band (Fermi resonance) or with a ligand-based vibration, which disappears upon ^{18}O-isotope shifting due to a frequency mismatch. To investigate possible coupling of ligand-based modes with the [$Cu_2(\mu$-$O)_2$]$^{2+}$ core vibration, we prepared [3,5-$(CF_3)_2$Ph($H_2L^{CH3,CD3}$)Cu(MeCN)], in which two of the four methyl groups (R″) were perdeuterated. UV−vis spectroscopic monitoring of the oxygenation of this complex at −80 °C in THF revealed a spectrum identical to that observed for the nondeuterated complex. An overlay of resonance Raman spectra of the deuterated and parent system ($^{16}O_2$ in Figure 11a; $^{18}O_2$ in Figure 11b) shows shifts upon ligand deuteration of bands at 467, 532, and 676 cm^{-1} that are not O-isotope sensitive. Thus, these bands are clearly associated with ligand-based vibrations, and their resonance enhancement supports attribution of the intense ∼380 nm absorption feature to a ligand-based $\pi \rightarrow \pi^*$ transition. Importantly, while the single band at 574 cm^{-1} in the $^{18}O_2$ spectrum is unperturbed within experimental error (±1 cm^{-1}) by ligand deuteration (Figure 11b), the feature at 586 cm^{-1} in the $^{16}O_2$ spectrum of the parent system shifts by 6 cm^{-1} upon deuterium substitution into the ligand methyl groups (Figure 11a). Although more complete studies would be necessary to quantify the effect, this result confirms that the O-isotope feature does mix with ligand vibrations and provides support for this mixing as one rationale for the complexity of the $^{16}O_2$ resonance Raman data. Similar effects have been noted for other bis(μ-oxo)dicopper compounds.[29b] Finally, we note the absence of any evidence for isomeric (μ-η^2:η^2-peroxo)dicopper species in the Raman spectra, consistent with the established tendency for systems supported by bidentated N-donor ligands to yield bis(μ-oxo) compounds.[2e,3,4b,30]

Conclusion

The combined UV−vis, EPR, O_2 uptake, and resonance Raman data indicate that the β-diketiminate Cu(I) complexes described herein react with O_2 at low temperature to form bis(μ-oxo)dicopper intermediates. These results contrast with those reported previously for the Cu(I) complexes of H(Me_2L^{iPr2})$^-$ and H(tBu_2L^{iPr2})$^-$,[9] which yield monomeric 1:1 Cu/O_2 adducts. This dichotomy may be rationalized by invoking differences in effective steric bulk of the ligands that are illustrated by the structural preferences of their Cu(II)−chloride compounds, [LCuCl]$_n$. The size of R″ [31] is one basis for these effects, as revealed by the proclivity of systems with R″ = Me or Et to yield dinuclear structures [LCuCl]$_2$ (which dissociate to some extent in solution) and [$L_2Cu_2(\mu$-$O)_2$]. The nature of the β-diketiminate backbone substituents also underlies the steric effects, however, as shown by the facts that (a) [Ph(H_2L^{iPr2})CuCl]$_2$ adopts a dinuclear structure whereas H(Me_2L^{iPr2})CuCl remains mononuclear and (b) Cu(I) complexes of ligands with R = aryl, R′ = H, and R″ = ^{i}Pr yield bis(μ-oxo)dicopper compounds upon oxygenation. In these cases the effective steric bulk of the R″ = ^{i}Pr group is modulated by the β-diketiminate backbone substituent pattern, whereby replacement of R′ = Me with R′ = H allows greater rotational flexibility of the ^{i}Pr group (cf. structures in Figure 7a,b). This flexibility

(31) Related steric arguments have been presented to rationalize differences in polymerization reactivity of β-diketiminate complexes of Zn(II); see ref 14.

enables greater access to the Cu center, which can adopt a 4-coordinate geometry and form binuclear complexes with single-atom bridges.

Experimental Section

General Considerations. All solvents and reagents were obtained from commercial sources and used as received unless noted otherwise. The solvents/reagents THF, pentane, CH_2Cl_2, toluene, and benzene were distilled from Na/benzophenone or passed through solvent purification columns (Glass Contour, Laguna, CA). Heptanes, hexamethyldisiloxane (HMDSO), CH_3CN, and Et_3N were distilled from CaH_2 under nitrogen. The concentration of ^{n}BuLi was determined by titration with diphenylacetic acid in THF prior to use. Labeled dioxygen ($^{18}O_2$) was obtained from Cambridge Isotopes, Inc., or Icon Isotopes, Inc. $H_2{}^{18}O_2$ was purchased from Icon Isotopes, Inc., as a 2.7% solution in H_2O, with 90% ^{18}O enrichment. The compounds 2-methyl-6-perdeuteriomethylaniline,[32] 2-phenyl-1,3-bis(dimethylamino)trimethinium hexafluorophosphate,[16] $[NO_2(H_2L^{Me2Me})H]$,[12] $[CuCH_2SiMe_3]_4$,[22] and $CuCl_2{\cdot}0.8THF$[18] were prepared as reported in the literature. All metal complexes were synthesized and stored in a Vacuum Atmospheres inert-atmosphere glovebox under a dry N_2 atmosphere or by using standard Schlenk and vacuum line techniques.

Physical Methods. NMR spectra were recorded on a Varian VI-300, VXR-300, JEOL FT-NMR Lambda 300WB, or Bruker Advance 600 spectrometer. Chemical shifts (δ) for ^{1}H and ^{13}C NMR spectra were referenced to residual protium in the deuterated solvent. UV−vis spectra were recorded on a HP8453 (190−1100 nm) diode array spectrophotometer. Low-temperature spectra were acquired using a custom-manufactured vacuum dewar equipped with quartz windows, with low temperatures achieved with the use of a low-temperature MeOH bath circulator or a Unisoku low-temperature UV−vis cell holder. Samples for EPR spectroscopy were prepared by bubbling O_2 through a solution of the Cu(I) complex (≈2.0 mM) at −80 °C in an EPR tube before freezing the solution in liquid nitrogen or by adding 2 equiv of H_2O_2/Et_3N at −60 °C in an EPR tube before incubating for 1 h and freezing the solution in liquid nitrogen. X-band EPR spectra were recorded on a Bruker E-500 spectrometer, with an Oxford Insruments EPR-10 liquid-helium cryostat (2−20 K, 9.61 GHz). Quantitation of EPR signal intensity for copper complexes was accomplished by comparing the double integration of the derivative spectrum to that of $[H(Me_2L^{iPr2})CuCl]$[7a] in 1:1 CH_2Cl_2/toluene. The EPR simulation was performed using the program EPR (F. Neese, University of Konstanz, Konstanz, Germany). Samples for resonance Raman spectroscopy were generated by bubbling $^{16}O_2$ through a solution of the Cu(I) complex (∼10 mM) at −80 °C, by freezing the solution at −196 °C and transferring ca. 10 mL of $^{18}O_2$ onto the solid and warming to −80 °C, or by adding 2 equiv of a 1:1 solution of 2.7% H_2O_2 (in H_2O) and Et_3N in THF. The starting complex concentrations were 10−15 mM in THF, toluene, or MeCN. Resonance Raman spectra were collected on an Acton 506 spectrometer using a Princeton Instruments LN/CCD-1100-PB/UVAR detector and ST-1385 controller interfaced with Winspec software. A Spectra-Physics 2030-15 argon ion laser with a power of 200 mW at the sample was employed to give the excitation at 457.9 nm. The spectra were obtained at −196 °C using a backscattering geometry; samples were placed in a Teflon cup and frozen by direct immersion in liquid nitrogen. Raman shifts were externally referenced to liquid indene. Cyclic voltammetry was performed using Pt working and auxiliary electrodes, a Ag wire reference electrode, and a BAS Epsilon potentiostat connected to a cell mounted in a Vacuum Atmospheres inert-atmosphere glovebox. All experiments were performed in MeCN with 0.1 M Bu_4NPF_6 at room temperature, and under these conditions the ferrocene/ferrocenium $E_{1/2} = +0.642$ V vs Ag wire. Elemental analyses were perfomed by Atlantic Microlab, Inc., or Oneida Research Services, Inc. Mass spectra were recorded with a JEOL JMS-700T tandem MS station, VG 7070-HF (FAB), or Finnigan MAT 95 MS station.

Magnetic Measurements. The overall magnetic moment M of $[Cl(Me_2L^{Me2})CuCl]_2$ was measured over the temperature range 5−300 K at four magnetic fields 0.5, 1, 2.5, and 5 T on a Quantum Design MPMS superconducting quantum interference device (SQUID) magnetometer. The sample (53 mg) was contained in a Kel F bucket which had been independently calibrated. The data were corrected for diamagnetism (-502×10^{-6} cm^3 mol^{-1}) using Pascal's constants.[33] The low-field data were simulated using the Van Vleck eq 1 derived from the Hamiltonian $\mathbf{H} = -2J\hat{S}_1\hat{S}_2 + \beta_e H\tilde{g}\hat{S}$,[33] with t being the temperature-independent paramagnetism (TIP) and the other parameters assigned their usual meaning.

$$\chi_m T \equiv \frac{M}{nH}T = 2\frac{N_A\beta_e^{\,2}}{k_B T}\, g^2 \frac{1}{3 + \exp\left(\frac{-2J}{kT}\right)} + 2tT \qquad (1)$$

2-(3,5-Bis(trifluoromethyl))phenyl-1,3-bis(dimethylamino)-trimethinium Hexafluorophosphate. 3,5-Bis(trifluoromethyl)-phenylacetic acid (17.7 g, 65.2 mmol) was placed in a three-necked round-bottomed flask, fitted with a dropping funnel and a reflux condenser, and purged with N_2. DMF (29 mL, 391 mmol) was added to the flask via syringe, and the solution was warmed to 70 °C. $POCl_3$ (10.0 g, 65.2 mmol) was placed in the dropping funnel and was added to the reaction mixture over approximately 2 h. After addition the crimson solution was heated at 70 °C for a further 3 h before being cooled to ambient temperature. A NaOH solution (35 mL of 5 M) and the reaction mixture were slowly and simultaneously added to a solution of HPF_6 (17.1 g, 10.4 mL, 60 wt % solution in H_2O), 5 M NaOH (18 mL), and H_2O (75 mL), while cooling in an ice bath and keeping $T < 10$ °C. After addition the solution was allowed to age for ca. 1 h while a yellow precipitate formed. The solution was filtered under vacuum, yielding a yellow solid. The solid was dissolved in the minimum of hot MeCN and filtered under vacuum. Excess Et_2O was added to the MeCN solution, which was placed at −20 °C overnight. Filtration of the solution under gravity yielded a yellow crystalline solid (13.4 g, 43%): ^{1}H NMR (CD_3CN, 300 MHz) δ 8.06 (s, 1H), 7.91 (s, 2H), 7.44 (s, 2H), 3.25 (s, 6H), 2.41 (s, 6H) ppm; $^{13}C\{^1H\}$ NMR (CD_3CN, 75 MHz) δ 164.23, 133.81, 132.30 (quartet, $J = 271$ Hz), 133.81, 124.41 (quartet, $J = 33.8$ Hz), 123.87, 103.11, 49.99, 41.47 ppm; FAB MS m/z 339.1301 ([M − PF_6]). Anal. Calcd for $C_{15}H_{17}N_2PF_{12}$: C, 37.19; H, 3.51; N, 5.79. Found: C, 36.89; H, 3.37; N, 5.72.

General Method for the Preparation of β-Diketimines.[16] The appropriate vinamidinium salt (typically 5 g, 13.2 mmol) was dissolved in EtOH (30 mL) and aqueous NaOH (30 mL of 25 wt %) and brought to reflux for approximately 45 min. After being cooled to ambient temperature, the biphasic solution was brought to pH 1 by the addition of 4 M HCl and extracted with Et_2O (2 × 100 mL). The organic fractions were combined, dried over $MgSO_4$, and filtered, and the solvent was removed under vacuum to yield a brown oil, which was used without further purification. A

(32) Eibler, E.; Käsbauer, J.; Pohl, H.; Sauer, J. *Tetrahedron Lett.* **1987**, *28*, 1097−1100.

(33) Kahn, O. *Molecular Magnetism*; VCH: New York, 1993.

quantitative yield for the hydrolysis was assumed for the β-diketimine syntheses. The brown oil was dissolved in EtOH (50 mL), and the desired aniline derivative (2.1 equiv) was added dropwise with 12 M HCl (1 equiv). The resulting solution was brought to reflux for approximately 1 h, cooled to ambient temperature, and then stirred overnight. The resulting brown solution was neutralized by the addition of excess $NaHCO_3$ and extracted with $CHCl_3$ (3×100 mL). The organic fractions were combined, dried over $MgSO_4$, and filtered, and the solvent was removed under vacuum to yield a brown oil. Recrystallization from MeOH yielded the product as a yellow crystalline solid in the indicated yield.

1-(2,6-Diisopropylphenyl)amino-3-(2,6-diisopropylphenyl)-imino-2-phenyl-1 -propene [Ph(H_2L^{iPr2})H]. Yield: 50%. ^{1}H NMR (C_6D_6, 300 MHz): δ 12.45 (br s, 1H), 7.05−7.82 (m, 11H), 7.73 (s, 2H), 3.45 (heptet, $J = 6.9$ Hz, 4H), 1.21 (d, $J = 6.9$ Hz, 12H) ppm. $^{13}C\{^1H\}$ NMR (C_6D_6, 75 MHz): δ 156.20, 144.40, 142.26, 140.82, 126.40, 125.78, 125.53, 124.11, 107.01 ppm. FAB MS: m/z 467.3414 ([M + H]$^+$). Anal. Calcd for $C_{33}H_{42}N_2$: C, 84.98; H, 9.01; N, 6.0. Found: C, 84.96; H, 9.23; N, 5.92.

1-(2,6-Diethylphenyl)amino-3-(2,6-diethylphenyl)imino-2-phenyl-1-propene [Ph(H_2L^{Et2})H]. Yield: 25%. ^{1}H NMR (C_6D_6, 300 MHz): δ 12.73 (br s, 1H), 7.84 (s, 2H), 7.31 (m, 5H), 7.16 (m, 6H), 2.77 (q, $J = 7.5$ Hz, 8H), 1.25 (t, $J = 7.5$ Hz, 12H) ppm. $^{13}C\{^1H\}$ NMR (C_6D_6, 75 MHz): δ 155.75, 145.63, 140.93, 137.41, 129.36, 127.44, 125.97, 125.84, 125.52, 107.28, 25.94, 15.61 ppm. FAB MS: m/z 411.2786 ([M + H]$^+$). Anal. Calcd for $C_{29}H_{34}N_2$: C, 84.88; H, 8.29; N, 6.83. Found: C, 84.94; H, 8.35; N, 6.78.

1-(2,6-Dimethylphenyl)amino-3-(2,6-dimethylphenyl)imino-2-phenyl-1-propene [Ph(H_2L^{Me2})H]. Yield: 33%. ^{1}H NMR (C_6D_6, 300 MHz): δ 12.04 (br s, 1H), 7.64 (s, 2H), 7.16 (m, 7H), 6.95 (m, 4H), 2.18 (s, 12H) ppm. $^{13}C\{^1H\}$ NMR (C_6D_6, 75 MHz): δ 155.25, 146.60, 141.01, 130.62, 129.30, 129.17, 126.16, 125.55, 125.04, 107.53, 19.37 ppm. FAB MS: m/z 355.2163 ([M + H]$^+$). Anal. Calcd for $C_{25}H_{26}N_2$: C, 84.75; H, 7.34; N, 7.91. Found: C, 84.43; H, 7.36; N, 7.88.

1-(2,6-Diisopropylphenyl)amino-3-(2,6-diisopropylphenyl)imino-2-(3,5-bis(trifluoromethyl))phenyl-1-propene [3,5-$(CF_3)_2$-C_6H_3(H_2L^{iPr2})H]. Yield: 20%. ^{1}H NMR (C_6D_6, 300 MHz): δ 12.74 (br. s, 1H), 7.67 (m, 3H), 7.65 (s, 2H), 7.14 (m, 6H), 3.38 (heptet, $J = 6.9$ Hz, 4H), 1.22 (d, $J = 6.9$ Hz, 24H) ppm. $^{13}C\{^1H\}$ NMR (C_6D_6, 75 MHz): δ 156.18, 143.31, 143.60, 143.31, 142.04, 132.76 (quartet, $J = 32.6$ Hz), 125.13, 124.42 (quartet, $J = 270.9$ Hz), 124.33, 118.76, 104.84, 29.21, 24.19 ppm. FAB MS: m/z 603.3182 ([M + H]$^+$). Anal. Calcd for $C_{35}H_{40}N_2F_6$: C, 69.77; H, 6.64; N, 4.65. Found: C, 69.71; H, 6.79; N, 4.66.

1-(2,6-Diethylphenyl)amino-3-(2,6-diethylphenyl)imino-2-(3,5-bis(trifluoromethyl))phenyl-1-propene [3,5-$(CF_3)_2C_6H_3$(H_2L^{Et2})H]. Yield: 25%. ^{1}H NMR (C_6D_6, 300 MHz): δ 12.70 (br. s, 1H), 7.77 (s, 2H), 7.68 (s, 1H), 7.32 (s, 2H), 7.18 (m, 6H), 2.73 (quartet, $J = 7.5$ Hz, 8H), 1.28 (t, $J = 7.5$ Hz, 12H) ppm. $^{13}C\{^1H\}$ NMR (C_6D_6, 75 MHz): δ 155.65, 144.75, 143.37, 132.58 (quartet, $J = 32.4$ Hz), 124.45 (quartet, $J = 271.1$ Hz), 123.33, 127.60, 126.34, 125.7, 118.75, 104.96, 25.79, 15.62 ppm. FAB MS: m/z 547.2567 ([M + H]$^+$). Anal. Calcd for $C_{31}H_{32}N_2F_6$: C, 68.13; H, 5.86; N, 5.13. Found: C, 68.01; H, 5.86; N, 5.07.

1-(2,6-Dimethylphenyl)amino-3-(2,6-dimethylphenyl)imino-2-(3,5-bis(trifluoromethyl))phenyl-1-propene [3,5-$(CF_3)_2C_6H_3$-(H_2L^{Me2})H]. Yield: 28%. ^{1}H NMR (C_6D_6, 300 MHz): δ 12.36 (br s, 1H), 7.63 (s, 1H), 7.51 (s, 2H), 7.37 (s, 2H), 6.94 (m, 6H), 2.11 (s, 12H) ppm. $^{13}C\{^1H\}$ NMR (C_6D_6, 75 MHz): δ 155.22, 145.74, 143.44, 132.49 (quartet, $J = 32.4$ Hz), 130.63, 129.29, 125.63, 124.46 (quartet, $J = 271.1$ Hz), 125.51, 118.78, 105.13, 19.21 ppm. FAB MS: m/z 491.1932 ([M + H]$^+$). Anal. Calcd for $C_{27}H_{24}N_2F_6$: C, 66.12; H, 4.90; N, 5.71. Found: C, 65.93; H, 5.01; N, 5.69.

1-(2-Methyl-6-trideuteriomethylphenyl)amino-3-(2-methyl-6-trideuteriomethylphenyl)imino-2-(3,5-bis(trifluoromethyl))-phenyl-1-propene, [3,5-$(CF_3)_2C_6H_3$($H_2L^{CH3,CD3}$)H]. Yield: 18%. ^{1}H NMR (C_6D_6, 300 MHz): δ 12.38 (br. s, 1H), 7.64 (s, 1H), 7.52 (s, 2H), 7.38 (s, 2H), 6.99 (s, 6H), 2.12 (s, 3H) ppm. $^{13}C\{^1H\}$ NMR (C_6D_6, 75 Mz): δ 155.21, 145.77, 143.45, 132.50 (quartet, $J = 32$ Hz), 130.62, 130.51, 129.30, 125.63, 125.50, 124.45 (quartet, $J = 272$ Hz), 118.78, 105.13, 19.18, 18.65 (heptet, $J = 20$ Hz). EI MS: m/z 496.2190 (M$^+$). Anal. Calcd for $C_{27}H_{18}D_6F_6N_2$: C, 65.32; H, 4.83; N, 5.65. Found: C, 65.10; H, 4.79; N, 5.56.

2-(2,6-Dimethylphenyl)amino)-4-((2,6-dimethylphenyl)imino-3-chloro-2-pentene, [Cl(Me_2L^{Me})H]. A 500 mL round-bottom flask was charged with a solution of 3-chloropentanedione (10.5 g, 78.3 mmol), 2,6-dimethylaniline (19.0 g, 157 mmol), and a catalytic amount of *p*-toluenesulfonic acid hydrate (approximately 0.50 g) in toluene (250 mL). The flask was equipped with a Dean−Stark apparatus, and the reaction mixture was refluxed under N_2 for 24 h, resulting in the development of a dark brown color. After the mixture was cooled to ambient temperature, the volatiles were removed under reduced pressure, yielding a dark brown oil. MeOH (150 mL) was added, yielding a suspension that was stirred for 30 min. The suspension was filtered to yield a tan powder, which was washed with cold MeOH (2×100 mL) and dried in vacuo. Recrystallization from the minimum amount of warm pentane yielded the product as tan crystals (2.18 g, 8.2%). ^{1}H NMR (C_6D_6, 300 MHz): δ 12.95 (br s, 1H), 6.94 (s, 6H), 2.02 (s, 12H), 1.90 (s, 6H) ppm. $^{13}C\{^1H\}$ NMR (C_6D_6, 75 MHz): δ 160.8, 144.0, 132.6, 128.7, 125.5, 19.0, 18.8 ppm. LREIMS: $m/z = 340$ (M$^+$). Anal. Calcd for $C_{21}H_{25}N_2Cl$: C, 73.99; H, 7.39; N, 8.22. Found: C, 74.17; H, 7.42; N 8.21.

[Ph(H_2L^{iPr2})Li·THF]. In an inert atmosphere ^{n}BuLi (0.43 mL, 1.0 equiv, 2.5 M in hexanes) was added dropwise to a stirred solution of [Ph(H_2L^{iPr2})H] (0.50 g, 1.07 mmol) in THF (5 mL). The golden yellow solution was stirred for approximately 30 min and the solvent removed under vacuum. The residue was dissolved in pentane (ca. 20 mL) and left at −20 °C overnight. Yellow crystals deposited, which were washed with cold pentane and dried in vacuo (0.463 g, 79%). ^{1}H NMR (C_6D_6, 300 MHz): δ 8.11 (s, 2H), 7.50 (m, 2H), 7.19 (m, 8H), 7.01 (m, 1H), 3.51 (heptet, $J = 6.9$ Hz, 4H), 3.26 (m, 4H), 1.23 (d, $J = 6.9$ Hz, 24H), 1.16 (m, 4H) ppm. $^{13}C\{^1H\}$ NMR (C_6D_6, 75 MHz): δ 161.80, 152.76, 145.72, 141.81, 129.08, 125.98, 124.24, 123.77, 123.26, 104.71, 68.45, 28.79, 25.10, 25.71, 23.99 ppm.

[Ph(H_2L^{Et2})Li]. In an inert atmosphere ^{n}BuLi (0.34 mL, 1.0 equiv, 2.5 M in hexanes) was added dropwise to a stirred solution of [Ph(H_2L^{Et2})H] (0.35 g, 0.85 mmol) in pentane (5 mL). The solution was stirred for approximately 30 min with the production of a cream precipitate. The solution was reduced in volume and was placed at −20 °C overnight. The solution was filtered under vacuum yielding a cream solid (0.33 g, 93%). ^{1}H NMR (C_6D_6, 300 MHz): δ 7.85 (s, 2H), 7.36 (m, 2H), 7.17 (m, 8H), 7.03 (m, 1H), 2.50 (quartet, $J = 7.5$ Hz, 8H), 1.18 (t, $J = 7.5$ Hz, 12H) ppm. $^{13}C\{^1H\}$ NMR (C_6D_6, 75 MHz): δ 161.16, 153.84, 145.30, 137.25, 128.99, 126.83, 125.83, 123.99, 123.34, 104.53, 26.05, 15.74 ppm.

[Ph(H_2L^{Me2})Li·THF]. In an inert atmosphere ^{n}BuLi (0.50 mL, 1.0 equiv, 2.5 M in hexanes) was added dropwise to a stirred solution of [Ph(H_2L^{Me2})H] (0.44 g, 1.24 mmol) in THF (5 mL). The solution was stirred for approximately 30 min and reduced in volume. A large excess of pentane was added, and the solution was placed at −20 °C overnight. The mother liquor was decanted

away from the brown crystals, which were washed with cold pentane and dried under vacuum (0.39 g, 73%). ^{1}H NMR (C_6D_6, 300 MHz): δ 8.09 (s, 2H), 700−7.49 (m, 11H), 3.29 (m, 4H), 2.34 (s, 12H), 1.18 (m, 4H) ppm. ^{13}C{^{1}H} NMR (C_6D_6, 75 MHz): δ 161.35, 155.46, 145.93, 130.80, 128.99, 128.89, 125.95, 123.07, 123.07, 105.07, 68.30, 25.71, 19.63 ppm.

[3,5-$(CF_3)_2C_6H_3(H_2Li^{Pr2})$Li]. In an inert atmosphere ^{n}BuLi (0.33 mL, 1.0 equiv, 2.5 M in hexanes) was added dropwise to a stirred solution of [3,5-$(CF_3)_2C_6H_3(H_2L^{iPr2})$H] (0.50 g, 0.83 mmol) in pentane (5 mL). The solution was stirred for approximately 30 min, with the production of a cream precipitate, reduced in volume, and placed at −20 °C overnight. The solution was filtered under vacuum to give a cream solid (0.44 g, 87%). ^{1}H NMR (C_6D_6, 300 MHz): δ 7.84 (s, 2H), 7.80 (s, 2H), 7.48 (s, 1H), 7.16 (m, 6H), 2.95 (heptet, J = 6.9 Hz, 4H), 1.15 (dd, J = 6.9 Hz, 24H) ppm. ^{13}C{^{1}H} NMR (C_6D_6, 75 MHz): δ 161.49, 151.34, 147.73, 141.31, 132.36 (quartet, J = 32.1 Hz), 125.04, 124.79 (quartet, J = 271.4 Hz), 124.43, 123.96, 116.16, 104.84, 28.93, 25.83, 23.29 ppm.

[3,5-$(CF_3)_2C_6H_3(H_2L^{Et2})$Li]. In an inert atmosphere ^{n}BuLi (0.22 mL, 1.0 equiv, 2.5 M in hexanes) was added dropwise to a stirred solution of [3,5-$(CF_3)_2C_6H_3(H_2L^{Et2})$H] (0.30 g, 0.55 mmol) in pentane (5 mL). The solution was stirred for approximately 30 min, with the production of a cream precipitate, reduced in volume, and placed at −20 °C overnight. The solution was filtered under vacuum to give a cream solid (0.27 g, 89%). ^{1}H NMR (C_6D_6, 300 MHz): δ 7.84 (s, 2H), 7.82 (s, 2H), 7.56 (s, 1H), 7.16−7.24 (m, 6H), 2.44 (quartet, J = 7.5 Hz, 8H), 1.18 (t, J = 7.5 Hz, 12H) ppm. ^{13}C{^{1}H} NMR (C_6D_6, 75 MHz): δ 161.01, 152.58, 147.71, 136.68, 132.25 (quartet, J = 31.6 Hz), 127.10, 126.34, 124.80 (quartet, J = 271.4 Hz), 124.57, 116.14 102.75, 25.89, 15.75 ppm.

[3,5-$(CF_3)_2C_6H_3(H_2L^{Me2})$Li]. In an inert atmosphere ^{n}BuLi (0.24 mL, 1.0 equiv, 2.5 M in hexanes) was added dropwise to a stirred solution of [3,5-$(CF_3)_2C_6H_3(H_2L^{Me2})$H] (0.30 g, 0.61 mmol) in pentane (5 mL). The solution was stirred for approximately 30 min, with the production of a pale yellow precipitate, reduced in volume, and placed at −20 °C. The solution was filtered under vacuum to give a pale yellow solid (0.29 g, 96%). ^{1}H NMR (C_6D_6, 300 MHz): δ 7.74 (s, 2H), 7.73 (s, 2H), 7.60 (s, 1H), 7.07−7.28 (m, 6H), 2.09 (s, 12H) ppm. ^{13}C{^{1}H} NMR (C_6D_6, 75 MHz): δ 160.60, 153.60, 147.66, 132.07 (quartet, J = 32.1 Hz), 130.42, 129.30, 124.82 (quartet, J = 271 Hz), 124.87, 124.04, 116.45, 103.42, 19.37 ppm.

[3,5-$(CF_3)_2C_6H_3(H_2L^{CH3,CD3})$Li]. In an inert atmosphere ^{n}BuLi (0.29 mL, 1.2 equiv, 2.5 M in hexanes) was added dropwise to a stirred solution of [3,5-$(CF_3)_2C_6H_3(H_2L^{CH3,CD3})$H] (0.30 g, 0.60 mmol) in pentane (5 mL). The solution was stirred for approximately 30 min, with the production of a pale yellow precipitate, reduced in volume, and placed at −20 °C. The solution was filtered under vacuum to give a pale yellow solid (0.23 g, 74%). ^{1}H NMR (C_6D_6, 300 MHz): δ 7.64 (s, 4H), 7.49 (s, 1H), 7.00 (m, 6H), 2.00 (s, 3H) ppm. ^{13}C{^{1}H} NMR (C_6D_6, 75 MHz): δ 160.69, 153.68, 147.70, 132.08 (quartet, J = 32.1 Hz), 130.40, 130.28, 128.98, 124.86, 124.83 (quartet, J = 271 Hz), 124.02, 116.15, 103.43, 19.39 ppm.

[Cl(Me_2L^{Me2})]Li·1.5THF. A solution of *n*-butyllithium (0.60 mL, 2.57 M in hexanes) was slowly added to a solution of [Cl(Me_2L^{Me2})H] (0.50 g, 1.47 mmol) in THF (5 mL). After the resulting brown solution was stirrred for 30 min, the volume was decreased to 2 mL under reduced pressure. Pentane (4 mL) was added, and the solution was stored at −20 °C overnight. Yellow crystals formed, which were washed with cold pentane (1 × 2 mL) and dried in vacuo. The supernatant was further concentrated and stored at −20 °C, resulting in the formation of a second crop of crystals (total yield = 0.35 g, 57%). ^{1}H NMR (C_6D_6, 300 MHz): δ 7.04 (d, 4H), 6.88 (t, 2H), 3.06−3.10 (m, 6H), 2.26 (s, 6H), 2.15 (s, 12H), 1.07−1.12 (m, 6H) ppm. ^{13}C{^{1}H} NMR (C_6D_6, 75 MHz): δ 162.46, 152.47, 130.95, 128.53, 122.48, 68.10, 25.66, 21.76, 19.25 ppm.

[Cl(Me_2L^{Me2})CuCl]$_2$. A solution of [Cl(Me_2L^{Me2})]Li·1.5 THF (0.512 g, 1.22 mmol) in THF (6 mL) was added to a slurry of $CuCl_2$·0.8 THF (0.235 g, 1.22 mmol) in THF (6 mL), causing the formation of a dark green color. The reaction mixture was stirred overnight, and the solvent was removed under reduced pressure. The green residue was extracted with CH_2Cl_2 (10 mL), yielding a purple solution that was filtered through a pad of Celite. The volume of solvent was reduced to 5 mL, HMDSO (5 mL) was added, and the solution was stored at −20 °C overnight, causing the deposition of dark crystals. The volume of the mother liquor was reduced and the solution stored at −20 °C, resulting in the formation of a second crop of crystals (total yield = 0.287 g, 54%). UV−vis (CH_2Cl_2) [λ_{max}, nm (ϵ, M^{-1} cm^{-1})]: 283 (5900), 327 (11 500), 362 (14 400), 505 (2500), 812 (600). Anal. Calcd for $C_{42}H_{48}N_4Cu_2Cl_2$: C, 57.47; H, 5.51; N, 6.38. Found: C, 57.56; H, 5.52; N, 6.36.

[H(Me_2L^{Et2})CuCl]$_2$. A solution of H(Me_2L^{Et})Li (0.390 g, 1.06 mmol) in THF (5 mL) was added to a slurry of $CuCl_2$·0.8THF (0.203 g, 1.06 mmol) in THF (5 mL), causing the development of a green-brown color. Manipulation as in the preparation of [Cl(Me_2L^{Me2})CuCl]$_2$ afforded the product as dark crystals (total yield = 0.255 g, 52%). UV−vis (CH_2Cl_2) [λ_{max}, nm (ϵ, M^{-1} cm^{-1})]: 283 (9800), 325 (15 100), 339 (13 800), 508 (3200), 640 (sh 800), 831 (500). Anal. Calcd for $C_{50}H_{66}Cu_2N_4Cl_2$: C, 65.20; H, 7.22; N, 6.08. Found: C, 64.87; H, 7.23; N, 6.01.

[Ph(H_2L^{iPr2})CuCl]$_2$. A solution of [Ph(H_2L^{iPr2})Li·THF] (0.176 g, 0.323 mmol) in THF (4 mL) was added to a slurry of $CuCl_2$·0.8THF (0.062 g, 0.323 mmol) in THF (4 mL), causing the development of a dark green color. The reaction mixture was stirred for 5 h, and the volatiles were removed under reduced pressure. The green residue was extracted with 6 mL of CH_2Cl_2, forming a deep brown-red solution that was filtered through a pad of Celite. The volume was reduced to 4 mL, and 2 mL of heptanes was added. Storage at −20 °C resulted in the deposition of green crystals. Addition of 2 mL of HMDSO to the mother liquor followed by cooling led to the formation of a second crop of crystals (total yield = 0.062 g, 34%). UV−vis (CH_2Cl_2) [λ_{max}, nm (ϵ, M^{-1} cm^{-1})]: 283 (21 100), 327 (8400), 379 (17 800), 514 (3000), 664 (sh, 1000), 837 (660). Anal. Calcd for $C_{66}H_{82}N_4Cu_2Cl_2$: C, 70.19; H, 7.32, N 4.96. Found: C, 70.39; H, 7.35; N, 4.99.

General Method for the Preparation of Cu(I) Complexes. In an inert atmosphere a solution of β-diketiminate lithium salt (0.1−1.0 mmol) in THF (2 mL) was added to a slurry of [Cu(MeCN)$_4$]CF_3SO_3 (1.0 equiv) in THF and stirred for 5 min. The solvent was removed under vacuum and the residue extracted with pentane (between 10 and 25 mL depending on complex formed) and filtered through a plug of Celite. The volume was reduced and the solution was placed at −20 °C overnight, yielding a yellow powder. The mother liquor was decanted away from the solid, which was dried under vacuum.

[H(Me_2L^{Et2})Cu(MeCN)]. This complex was isolated from pentane at −20 °C to give a yellow powder (57%). Drying under vacuum resulted in the loss of coordinated MeCN. ^{1}H NMR (C_6D_6, 300 MHz): δ 7.15 (m, 6H), 4.82 (s, 1H), 2.46 (q, J = 7.5 Hz, 8H), 1.70 (s, 6H), 1.15 (t, J = 7.5 Hz, 12H) ppm. Anal. Calcd for $C_{25}H_{33}N_2Cu$: C, 70.67; H, 7.77; N, 6.60. Found: C, 71.41; H, 7.64; N, 7.20.

[H(Me_2L^{Me2})Cu(MeCN)]. This complex was isolated from pentane at −20 °C to give a yellow powder (40%). Drying under

vacuum resulted in the loss of coordinated MeCN. ^{1}H NMR (C_6D_6, 300 MHz): δ 7.13 (m, 4H), 6.99 (m, 2H), 4.79 (s, 1H), 2.03 (s, 12H), 1.65 (s, 6H) ppm. Anal. Calcd for $C_{25}H_{33}N_2Cu$: C, 68.39; H, 6.78; N, 7.60. Found: C, 68.96; H, 7.07; N, 7.28.

[Ph(H$_2$L^{iPr2})Cu(MeCN)]. This complex was recrystallized from pentane at −20 °C to give a yellow crystalline solid (60%). ^{1}H NMR (C_6D_6, 300 MHz): δ 8.00 (s, 2H), 7.36 (d, J = 7.5 Hz, 8H), 7.15 (m, 8H), 7.00 (t, J = 7.5 Hz, 1H), 3.34 (heptet, J = 6.9 Hz, 4H), 1.18 (d, J = 6.9 Hz, 12H), 1.05 (d, J = 6.9 Hz, 12H), 0.27 (s, 3H) ppm. Anal. Calcd for $C_{35}H_{44}N_3Cu$: C, 73.71; H, 7.54; N, 7.39. Found: C, 73.71; H, 7.78; N, 7.37.

[Ph(H$_2$L^{Et2})Cu(MeCN)]. This complex was isolated from pentane at −20 °C to give a yellow powder (51%). Drying under vacuum resulted in the loss of coordinated MeCN. ^{1}H NMR (C_6D_6, 300 MHz): δ 7.94 (s, 2H), 7.04−7.31 (m, 11H), 2.56 (m, 8H), 1.15 (t, J = 7.5 Hz, 12H) ppm. Anal. Calcd for $C_{29}H_{33}N_2Cu$: C, 73.62; H, 7.03; H, 5.92. Found: C, 73.76; H, 6.99; N, 5.89.

[Ph(H$_2$L^{Me2})Cu(MeCN)]. This complex was isolated from pentane at −20 °C to give a yellow powder (31%). Drying under vacuum resulted in the loss of coordinated MeCN. ^{1}H NMR (C_6D_6, 300 MHz): δ 7.81 (s, 2H), 7.02−7.19 (m, 11H), 2.09 (s, 12H) ppm. Anal. Calcd for $C_{25}H_{25}N_2Cu$: C, 72.00; H, 6.04; N, 6.71. Found: C, 72.02; H, 6.00; N, 6.72.

[3,5-(CF$_3$)$_2$C$_6$H$_3$(H$_2$L^{iPr2})Cu(MeCN)]. This complex was recrystallized from pentane at −20 °C to give a yellow crystalline solid (55%). ^{1}H NMR (C_6D_6, 300 MHz): δ 8.01 (s, 2H), 7.84 (s, 2H), 7.52 (s, 1H), 7.17 (m, 6H), 3.50 (heptet, J = 6.9 Hz, 4H), 1.29 (d, J = 6.9 Hz, 12H), 1.19 (d, J = 6.9 Hz, 12H), 0.20 (s, 3H) ppm. Anal. Calcd for $C_{37}H_{42}N_3F_6Cu$: C, 62.93; H, 5.95; N, 5.95. Found: C, 62.87; H, 6.05; N, 5.91.

[3,5-(CF$_3$)$_2$C$_6$H$_3$(H$_2$L^{Et2})Cu(MeCN)]. This complex was isolated from pentane at −20 °C to give a yellow powder (56%). Drying under vacuum resulted in partial loss of MeCN (0.3 equiv remaining). ^{1}H NMR (C_6D_6, 300 MHz): δ 7.92 (s, 2H), 7.80 (s, 2H), 7.60 (m, 1H), 7.19−7.23 (m, 6H), 2.60 (m, 8H), 1.21 (t, J = 7.5 Hz, 12H), 0.37 (s, 1H) ppm. Anal. Calcd for $C_{31}H_{31}N_2F_6Cu\cdot 1/3CH_3CN$: C, 61.08; H, 5.14; N, 5.25. Found: C, 61.16; H, 5.03; N, 5.17.

[3,5-(CF$_3$)$_2$C$_6$H$_3$(H$_2$L^{Me2})Cu(MeCN)]. This complex was isolated from pentane at −20 °C to give a yellow powder (25%). Drying under vacuum resulted in loss of MeCN. ^{1}H NMR (C_6D_6, 300 MHz): δ 7.78 (s, 2H), 7.70 (s, 2H), 7.65 (s, 1H), 7.08−7.28 (m, 6H), 2.17 (s, 12H) ppm. Anal. Calcd for $C_{27}H_{23}N_2F_6Cu$: C, 58.64; H, 4.19; N, 5.07. Found: C, 59.12; H, 4.11; N, 4.95.

[3,5-(CF$_3$)$_2$C$_6$H$_3$(H$_2$L^{CH3,CD3})Cu(MeCN)]. This complex was isolated from pentane at −20 °C to give a yellow powder (46%). Drying under vacuum resulted in loss of MeCN. ^{1}H NMR (C_6D_6, 300 MHz): δ 7.63 (s, 2H), 7.56 (s, 2H), 7.53 (s, 1H), 7.02 (m, 6H), 2.00 (s, 6H) ppm. Anal. Calcd for $C_{27}H_{23}N_2F_6D_6Cu$: C, 58.01; H, 4.12; N, 5.01. Found: C, 57.75; H, 3.99; N, 4.84.

[Cl(Me$_2$L^{Me2})Cu(CNC$_6$H$_3$Me$_2$)]. A solution of Cl(Me$_2$L^{Me2})H (0.200 g, 0.587 mmol) in THF (10 mL) was treated with [CuCH$_2$SiMe$_3$]$_4$ (0.088 g, 0.587 mmol) and 2,6-dimethylphenyl 1-isocyanide (0.077 g, 0.587 mmol), causing the formation of a yellow solution. The reaction mixture was stirred for 30 min, and the solvent was removed in vacuo to yield a light brown solid. This solid was taken up in Et$_2$O (15 mL), the solution was filtered, and the solvent volume was reduced to 10 mL. Storage of the filtrate at −20 °C overnight led to the deposition of light yellow crystals that were isolated and dried under reduced pressure (0.132 g, 42%). ^{1}H NMR (C_6D_6, 300 MHz): δ 7.05 (d, J = 7.5 Hz, 4H), 6.92 (t, J = 7.5 Hz, 2H), 6.58 (t, J = 7.5 Hz, 1H), 6.37 (d, J = 7.5 Hz, 2H), 2.31 (s, 12H), 2.21 (s, 6H), 1.57 (s, 6H) ppm. ^{13}C{^{1}H} NMR (C_6D_6, 75 MHz): δ 162.7, 153.2, 135.4, 130.4, 129.0, 128.8, 127.9, 123.3, 102.7, 21.5, 19.7, 18.4 ppm. UV−vis (THF) [λ_{max}, nm (ϵ, M^{-1} cm^{-1}): 359 (25 000). FTIR (KBr, cm^{-1}): 2128 (ν_{CN}). Anal. Calcd for $C_{30}H_{33}N_3ClCu$: C, 67.40; H, 6.22; N, 7.86. Found: C, 67.55; H, 6.43; N, 7.58.

[{NO$_2$(H$_2$L^{Me2Me})Cu}$_2$(μ-OH)$_2$]. An anaerobic MeCN solution (10 mL) containing [NO$_2$(H$_2$L^{Me2Me})Cu(MeCN)] (41 mg, 0.1 mmol based on cuprous ion) was prepared by dissolving the polymer [NO$_2$(H$_2$L^{Me2Me})Cu]$_x$.[12] Dry O_2 was introduced into the solution by bubbling it through a needle at −40 °C for several min. The color of the solution turned from pale yellow to dark brown. The solution was allowed to stand for several h at −40 °C and then warmed to room temperature. Removal of the solvent by evaporation gave a residue, which was recrystallized from CH_2Cl_2 to give the product (38 mg, 87%). UV−vis (MeCN) [λ_{max}, nm (ϵ, M^{-1} cm^{-1})]: 353 (33 100). FTIR (KBr, cm^{-1}): 3638, 1613, 1601, 1530, 1296. Anal. Calcd for $C_{42}H_{50}N_6O_6Cu_2$: C, 58.52; H, 5.85; N, 9.75. Found: C, 58.27; H, 5.82; N, 9.62.

Spectrophotometric O_2 Titrations. A 4 mL sample of a stock solution of [Ph(H$_2$L^{iPr2})Cu(MeCN)] in THF (0.25 mM) was placed in a UV−vis cuvette and cooled to −80 °C, and the headspace of the cuvette was evacuated. Spectra were taken before and after to ensure that no sample degradation had occurred. Using a syringe, either 1.0, 0.75, 0.5, or 0.25 equiv of O_2 (by volume of 1% O_2 in N_2 gas) was injected into the cuvette where it was left to equilibrate, with occasional mild agitation. The progress of oxygenation was followed by monitoring the shoulder at 433 nm in the UV−vis spectrum. In each case, the reaction was run until no further increase in absorbance at 433 nm was observed. Measured absorbance values of 1.09, 1.08, 1.01, and 0.69, respectively, were consistent with a Cu:O_2 stoichiometry of 2.0(2):1.

X-ray Crystallography. Crystal data and collection parameters are listed in Table 2. A crystal of the appropriate size (with one exception; see Supporting Information for full information in the form of CIFs) was mounted on a glass fiber using fluorinated oil and transferred to either a Siemens or Bruker SMART diffractometer/CCD area detector or a Rigaku RAXIS-RAPID imaging plate two-dimensional area detector. The crystal was centered in the X-ray beam (Mo Kα radiation; λ = 0.710 73 Å, graphite monochromator) for data collection. The intensity data were corrected for Lorentz polarization effects (SAINT)[34] and absorption [SADABS,[35] XPREP,[36] or the crystal structure software from the Molecular Structure Corp. (CSS-MSC)[37]]. The structure was solved by direct methods using SHELXS-97,[38] SIR92,[39] or CSS-MSC,[37] which provided most non-hydrogen atoms. Full-matrix least-squares/difference Fourier cycles were performed using SHELXL-97,[38] which located the remaining non-hydrogen atoms. All non-hydrogen atoms were refined with anisotropic displacement parameters. All hydrogen atoms were placed in ideal positions and refined as riding atoms with isotropic displacement parameters related to the parent atom. Pertinent details for each structure are noted below; see Supporting Information for full information in the form of CIFs.

(34) *SAINT V6.01*; Bruker Analytical X-ray Systems: Madison, WI, 1999.
(35) An empirical correction for absorption anisotropy: Blessing, R. *Acta Crystallogr.* **1995**, *A51*, 33−38.
(36) *Bruker Data Preparation & Reciprocal Space Exploration*, ver. 5.1; Bruker-AXS, Inc.: Madison, WI, 1997.
(37) *Crystal Structure Analysis Package*, version 2.0; Molecular Structure Corp. and Rigaku Corp: The Woodlands, TX, 2001.
(38) *SHELXTL-Plus*, V5.10, Bruker Analytical X-ray Systems: Madison, WI, 1997.
(39) Altomare, A.; Cascarno, G.; Giacovazzo, C.; Gualardi, A. SIR92. *J. Appl. Crystallogr.* **1993**, *26*, 343−350.

[Ph(H$_2$L^{iPr2})Cu(MeCN)]. Crystals suitable for X-ray crystallographic analysis were grown from pentane at −20 °C. The carbon atoms of one isopropyl group were found to be disordered over two positions, with a 63:37 occupancy ratio.

[3,5-(CF$_3$)$_2$C$_6$H$_3$(H$_2$L^{iPr2})Cu(MeCN)]. Crystals suitable fo r X-ray crystallographic analysis were grown from pentane at −20 °C. The carbon atoms of one isopropyl group were found to be disordered over two positions, each with a 75:25 occupancy ratio. The fluorine atoms of one of the CF_3 groups were found to be disordered over four positions. The C−F and F−F distances were restrained to be equal. The MeCN was found to be disordered over two positions, with an 84:16 occupancy ratio.

[Cl(Me$_2$L^{Me2})Cu(CNC$_6$H$_3$Me$_2$)]. Crystals suitable for X-ray crystallographic analysis were grown from pentane at −20 °C overnight. The last 21 frames of data collection were omitted due to the presence of a much higher background than all other frames (presumably due to water condensation on the collimator).

[Cl(Me$_2$L^{Me2})CuCl]$_2$. Crystals suitable for X-ray crystallographic analysis were grown by vapor diffusion of pentane into a CH_2Cl_2 solution of the complex at −20 °C.

[H(Me$_2$L^{Et2})CuCl]$_2$. Crystals suitable for X-ray crystallographic analysis were grown from a mixture of CH_2Cl_2 and HMDSO at −20 °C. Data were collected at room temperature, since cooling significantly below ambient temperature induced splitting of the crystals. The chloride bridges are disordered over two sets of positions in an 85:15 ratio. One of the ethyl groups is also disordered, with the terminal methyl group occupying two positions in a 65:35 ratio.

[{NO$_2$(H$_2$L^{Me2}Me)Cu}$_2$(μ-OH)$_2$]. Crystals suitable for X-ray crystallographic analysis were grown from pentane diffusion into CH_2Cl_2 at −20 °C. The hydroxyl hydrogen atoms were located in difference maps, and their positions were refined.

Acknowledgment. We thank Professor Lawrence Que, Jr., and Dr. Raymond Ho for assistance with resonance Raman spectroscopy, Professor John Lipscomb for access to his EPR spectrometer, Lynneice Bowen for initial synthetic contributions, and Nermeen Aboelella for assistance with X-ray crystallography. Funding for this research was provided by the National Institutes of Health (Grant GM47365 to W.B.T.), the National Science Foundation (predoctoral fellowship to A.M.R.), and the Japanese Ministry of Education, Science, Culture, and Sports (Grants 11228206 and 13480189 to S.I.).

Supporting Information Available: Plots of magnetic susceptibility data as a function of temperature for [Cl(Me$_2$L^{Me2})CuCl]$_2$ at varying applied magnetic fields (Figure S1), UV−vis spectra of [Ph(H$_2$L^{iPr2})CuCl]$_2$ at different temperatures (Figure S2), cyclic voltammograms of [Ph(H$_2$L^{iPr2})Cu(MeCN)] (Figure S3), resonance Raman spectra of solutions of the intermediates resulting from the reactions of Cu(I) complexes with $^{16}O_2$ and $^{18}O_2$ (Figure S4), and complete X-ray crystallographic data as CIFs. This material is available free of charge via the Internet at http://pubs.acs.org.

IC020369K